

USING A LOW COST SOFTWARE DEFINED RADIO AS A WIND PROFILING RADAR RECEIVER

A Project Report

submitted by

P YASODHA

in partial fulfilment of the requirements

for the award of the degree of

MASTER OF TECHNOLOGY



DEPARTMENT OF ELECTRICAL ENGINEERING

INDIAN INSTITUTE OF TECHNOLOGY MADRAS

MAY 2014

CERTIFICATE

This is to certify that the thesis titled **“USING A LOW COST SOFTWARE DEFINED RADIO AS A WIND PROFILING RADAR RECEIVER”**, submitted by **POLISETTI YASODHA**, to the Department of Electrical Engineering, Indian Institute of Technology, Madras, for the award of the degree of **MASTER OF TECHNOLOGY**, is a bonafied record of the work done by her under my supervision. The contents of this thesis, in full or in parts, have not been submitted to any other institute or university for the award of any degree or diploma.

Dr Devendra Jalihal,
Project Advisor,
Professor,
Dept of Electrical Engineering
IIT Madras, 600 036

Place: Chennai

Date: May 6th, 2014

ACKNOWLEDGEMENTS

First and foremost I am deeply indebted to my guide Prof. Devendra Jalihal, for his valuable guidance and continuous support throughout this project. His suggestions at every stage in the work has boosted my confidence and helped me in achieving the progress in work. I am honoured and encouraged to work under his guidance.

I express my sincere gratitude to Dr P Srinivasulu, Sci/Engineer SG, Head, RADG, NARL, for his continuous support and guidance in completing this project. I would like to thank Prof A Jayaraman, Director, NARL, and Sri K V Lakshmana Kumar, Sr ADO, NARL for their support in sponsoring me to pursue M Tech at IIT Madras. I also would like to thank my colleagues Sri K Jayaraj, who helped me in conducting the experiments with LAWP radar, Sri M Durga Rao and Sri P Kamaraj for their support in completing the work.

I would like to thank my classmates and friends at IIT Madras, who have helped me directly or indirectly in completing the work.

Finally, I thank my family members, who have taken all the pains to send me to IIT Madras and without whose support and encouragement I could have not completed this work. I dedicate my work to them.

P YASODHA

ABSTRACT

Aim of the proposed work is to develop a low cost software defined radio (SDR), which can be used to observe a wide range of spectrum and use it as a wind profiling radar receiver. The basic mother boards for software defined radio peripherals cost about \$ 500 whereas the daughter boards cost about \$ 200. This has been greatly reduced to about \$ 40 with the use of the demodulator chip which is intended for decoding HDTV broadcasting. This cheaper demodulator chip can be used as the radar receiver.

The signal received by the radar antenna is amplified in the low noise amplifier and is given to low cost SDR. The SDR contains a tuner whose frequency range depends on the application and a demodulator chip, which is made with the HDTV broadcasting demodulator, delivers the digital data output for further data processing.

The demodulator chip is Taiwan's Realtek make RTL2832U. This is intended for decoding European HDTV broadcasting and it is an USB dongle type receiver, making it very simple to interface with any PC. This chip can deliver the raw digital data output (inphase and quadrature phase components of the received signal), over a wide range of frequencies. This raw data can be further processed, resulting in a low cost software defined radio that can pick up a huge variety of transmissions with different modulation schemes. But the disadvantage with this chip is that it is not as sensitive as purpose built SDRs. To overcome this, a low noise amplifier is used just after the antenna to increase the sensitivity level of the SDR.

After successfully developing the receiver it is proposed to develop multiple numbers (about 6), which can be used for atmospheric radars. The raw data obtained from the six channels can be processed for digital beam forming (DBF), post beam steering (PBS), imaging etc.

LIST OF FIGURES

Figure-1.1: Phase shifting of the received signal	2
Figure-1.2: Doppler Beam Swinging (DBS) Technique	3
Figure-2.1: Block Diagram of MST Radar	6
Figure-2.2: Photograph of MST Radar	6
Figure-2.3: Typical range-Doppler Spectra obtained in five beam directions	8
Figure-2.4: Block diagram of LAWP radar	10
Figure-2.5: Photograph of the LAWP Radar	11
Figure-2.6: Typical range-Doppler spectra	13
Figure-3.1: Data processing sequence	14
Figure-3.2: Range gating	14
Figure-3.3: Range-bin wise coherent integration	15
Figure-3.4: Coherent integration for a single range-bin: an example	16
Figure-3.5: Incoherent integration	17
Figure-3.6: Typical Doppler power spectrum for a single range-bin	17
Figure-5.1: Photograph of RTL2832U demodulator	20
Figure-6.1: GNU Radio companion (GRC)	23
Figure-7.1: Block diagram of the setup	24
Figure-7.2: GRC flow graph to monitor the frequency spectrum	24
Figure-7.3: GUI for parameter adjustment	25
Figure-7.4 a: Spectrum showing FM Radio stations at 92.7 MHz and 93.4 MHz observed at Tirupati, Andhra Pradesh	25
Figure-7.4 b: Spectrum showing a pulsed RF signal at 480 MHz observed at Tirupati, Andhra Pradesh	26
Figure-7.5: PHOTO of set-up	26
Figure-7.6: FM Radio receiver flow graph	27

Figure-7.7a: Block diagram for the signal generator experiment	29
Figure-7.7b: Photograph of the signal generator experiment	29
Figure-7.8: Base-band signal output showing the frequency difference between signal generator and RTL2832U demodulator.	30
Figure-7.9: Scope plot of GRC after adjusting the frequency in signal generator (set to 70.00182 MHz)	31
Figure-7.10a: Base-band output for simulated 70 MHz pulsed RF	31
Figure-7.10b: Base-band output for simulated 1280 MHz pulsed RF with pulse width equal to 4 μ s. Nulls can be observed in the spectrum at 0.25 MHz corresponding to 4 μ s.....		32
Figure-7.11: Flow graph for radar experiment	34
Figure-7.12a: I (top) and Q (bottom) plots indicating spurious spikes in the processed data	35
Figure-7.12b: Range-Doppler spectra for the data processed	36
Figure-7.13a: I (top) and Q (bottom) plots indicating spurious spikes in the processed data	38
Figure-7.13b: Range-Doppler spectra for the data processed	39
Figure-7.14: Raw base-band output of the simulated signal experiment, showing a sinusoidal signal modulating	39
Figure-7.15: Base-band output of the simulated signal experiment indicating the start of first pulse.	40
Figure-7.16: Base-band output of the simulated signal experiment showing the offset in timing	40
Figure-7.17: In-built crystal is replaced by an external clock. Figure also shows the replacement of the RF connector with an SMA connector.	41
Figure-7.18: GRC screen when the RTL2832U is fed with external clock. No output in scope plot.	41

LIST OF TABLES

Table-2.1: Specifications of MST Radar	7
Table-2.2: Specifications of LAWP radar	12
Table-7.1: Experimental specifications	34

CONTENTS

1. Introduction
2. Wind Profiling radars at NARL
3. Data processing
4. Need for low cost radars/subsystems
5. RTL2832UL: The low cost SDR
6. GNU Radio
7. Approach for realization
 - Initial experiments
 - Experiments with signal generator
 - Experiments with radar
 - Simulated signal experiments with signal generator
- Conclusion
- Future scope
- References

CHAPTER-1

Introduction

Observations of wind velocity profiles are very important for studying meteorological phenomena and weather forecasting. Atmospheric radar, also called as wind profiling radar, a coherent-pulse-Doppler-radar, is one of the most suitable remote sensing instruments for observing height profiles of three components of wind velocity vector, including the vertical velocity, with high time and height resolutions without influence of weather conditions.

Electromagnetic (EM) wave propagation is affected by the refractive index (RI) of the atmosphere. The RI is a measure of speed at which EM waves propagate through a medium. A spatial variation in RI encountered by EM wave causes a minute amount of the energy to be scattered in all directions. In the atmosphere, minor irregularities in the RI exist over a wide range of sizes. RI depends primarily upon the temperature, pressure and humidity of the atmosphere. The atmosphere is in a constant state of agitation, which produces irregular, small scale variations in the temperature and moisture over relatively short distances. The wind, as it varies in direction and speed, produces turbulent eddies, which produce variations in the refractive index of air that initiate scattering. As the irregularities in refractive index are carried by the wind, they prove to be good tracers of wind.

The electromagnetic pulse radiated by the radar is scattered due to the random irregularities present in the refractive index of the atmosphere. Back scattered echoes, which are shifted in phase compared to the transmitted signal, as shown in figure-1.1, are received by the radar and are analysed for their intensity and Doppler shifts.

Atmospheric radars derive information on the dynamical atmospheric phenomenon by making use of variations in amplitude and frequency of radio waves which are transmitted from radar system, back scattered by the atmosphere and received by the radar system again.

Doppler beam swinging (DBS) technique is used in wind profiling radars to derive the wind vector. In this technique the narrow radar beam is switched in three or five non-coplanar directions, as shown in figure-1.2, in a fixed sequence. The intensity and Doppler frequency

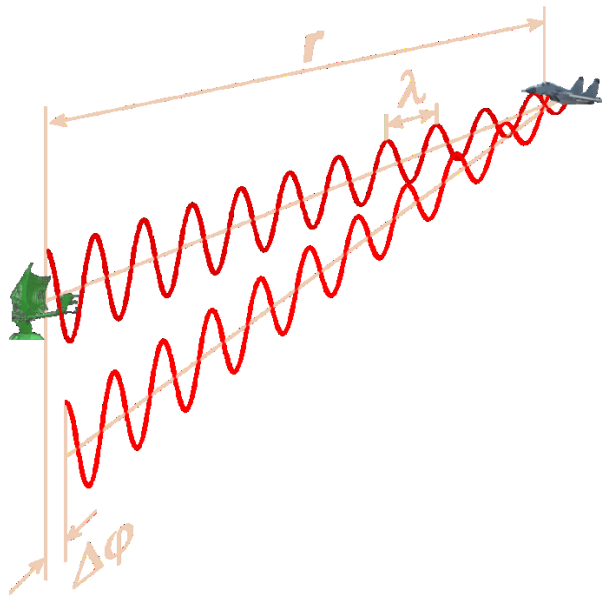
shift (f_d) measured in three (or more) radial directions are used to derive the wind vector of the atmosphere.

$$\text{Radial velocity of the wind } V_D = f_d * (\lambda/2)$$

The radial velocities obtained in all beam directions are used to compute the three components of the winds as follows

$$\begin{bmatrix} V_x \\ V_y \\ V_z \end{bmatrix} = \begin{bmatrix} \sum_i \cos^2 \theta_{xi} & \sum_i \cos \theta_{xi} \cos \theta_{yi} & \sum_i \cos \theta_{xi} \cos \theta_{zi} \\ \sum_i \cos \theta_{xi} \cos \theta_{yi} & \sum_i \cos^2 \theta_{yi} & \sum_i \cos \theta_{yi} \cos \theta_{zi} \\ \sum_i \cos \theta_{xi} \cos \theta_{zi} & \sum_i \cos \theta_{yi} \cos \theta_{zi} & \sum_i \cos^2 \theta_{zi} \end{bmatrix}^{-1} * \begin{bmatrix} V_{Di \cos \theta_{xi}} \\ V_{Di \cos \theta_{yi}} \\ V_{Di \cos \theta_{zi}} \end{bmatrix}$$

Where θ_{xi} , θ_{yi} , θ_{zi} are angles of i^{th} beam with X, Y and Z axis respectively and V_{Di} is the radial wind measured in beam direction i .

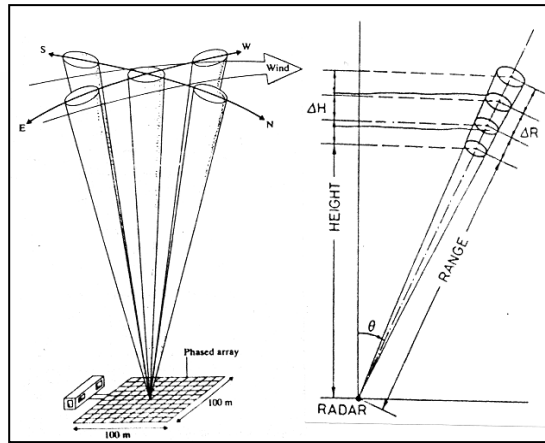


$$\omega_d = \frac{d\phi}{dt} = \frac{4\pi}{\lambda} \frac{dR}{dt} = \frac{4\pi}{\lambda} v_r$$

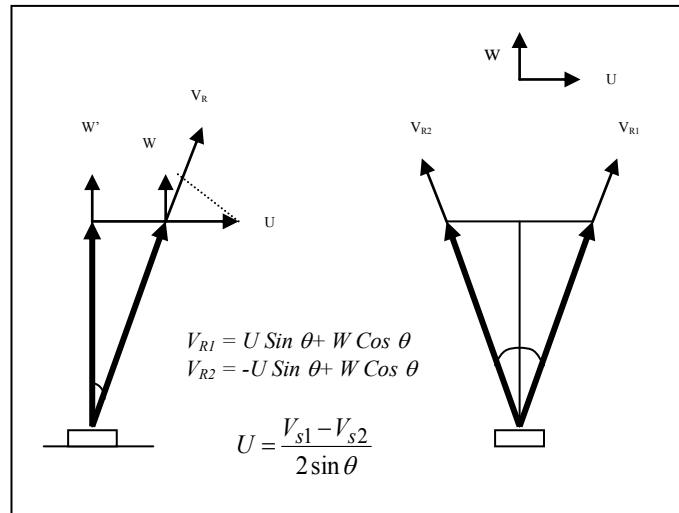
$$f_d = \frac{2}{\lambda} v_r$$

Figure-1.1: Phase shifting of the received signal

- DBS method for wind vector calculations (u, v, w)
- radial scattered velocities measured with one vertical and 2 (4) off-zenith beams
- beam-pointing sequence is repeated every 1-5 minutes
- Electronic beam pointing with phase shifters using one antenna
- local horizontal uniformity of the wind field is assumed



Radar beam geometry for DBS mode of operation



Typical beam directions used in DBS observations

Figure-1.2: Doppler Beam Swinging (DBS) Technique

DBS technique operates with the assumption of local horizontal uniformity of the wind field over the spatial separation of the beams (i.e. uniform background atmosphere). However, this assumption is not valid, for the case of disturbed atmosphere (convection/precipitation etc) and thus DBS technique is not appropriate for such cases. Complementary techniques like spaced antenna (SA), spatial domain interferometry (SDI), coherent radar imaging (CRI) are essential to study such events.

Wind profiling radars at National Atmospheric Research Laboratory are described in Chapter-2. Data Processing used in wind profiling radars is described in Chapter-3. Need for low cost

radars/subsystems is explained in chapter-4. The heart of this work, RTL2932U and GNU Radio are described in chapter-5 and 6 respectively. Realisation approach is explained in chapter-7, followed by conclusion and future scope.

CHAPTER-2

Wind Profiling radars at NARL

Details of the wind profiling radars located at National Atmospheric Research Laboratory (NARL), Department of Space, Government of India, Gadanki, are given below.

Mesosphere-Stratosphere-Troposphere (MST) radar

NARL has a state-of-the-art Pulsed, Doppler, Coherent Mesosphere-Stratosphere-Troposphere (MST) Radar, operating at 53 MHz, with a peak power aperture product of $2.5 \times 10^{10} \text{ W-m}^2$, which has a phased antenna array of 1024 crossed three element yagi-uda antennas arranged in a 32×32 matrix (square grid) over an area of $130 \text{ m} \times 130 \text{ m}$. The Radar has 32 distributed transmitters of varying powers, from 120 kW down to 15 kW, each one feeding a linear sub array of 32 antennas, via a dual directional coupler and a duplexer. The duplexer, realized using 90° hybrids and PIN diodes as the switching elements, connects the linear sub array to a receive channel, in the receive mode. The signals from 32 receive channels after amplification and down conversion are combined and the resulting IF signal is amplified and band-limited. Then the signal is given to a quadrature demodulator and the resulting in-phase (I) and quadrature-phase (Q) signals are passed through LPFs (Matched filters) and video amplifiers, which raise the signals to a level sufficient for further processing.

The base-band I and Q signals are first sampled at 1 MHz rate and digitized. The data is then decoded, where it is cross correlated with the replica of the transmitted signal. The I and Q data is coherently averaged to improve SNR. The time series data is then converted into frequency domain by applying complex Fourier transform, to obtain the range-Doppler spectra. The data is then processed (off-line) to obtain the three moments, which are signal power, mean Doppler frequency shift and the Doppler width. Mean Doppler frequency is used to obtain the three components of the wind vector.

The block diagram and photograph of MST radar are shown in figure-2.1 and figure-2.2 respectively. Important specifications of the radar are given in table-2.1. Typical range-Doppler spectral plots obtained are shown in figure-2.3.

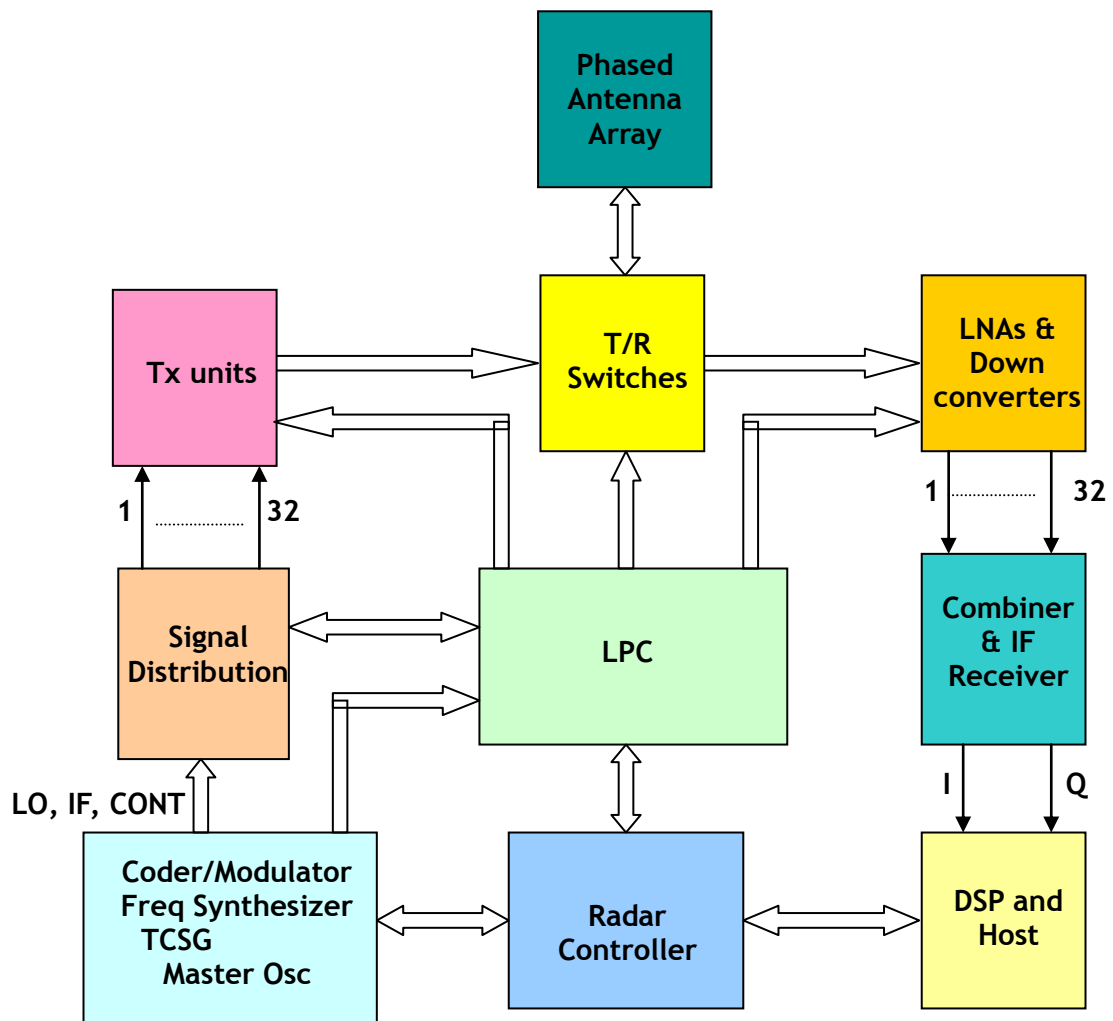


Figure-2.1: Block Diagram of MST Radar



Figure-2.2: Photograph of MST Radar

Parameter	value
Frequency	: 53 MHz
Antenna type	: 3-element Yagi
Array size	: 32x32
Beam Width	: 3°
Peak Power	: 2.5 MW
Maximum Duty Ratio	: 2.5 %
Pulse width	: 1 to 32 μ s
Pulse repetition frequency	: 62.5 Hz to 8 kHz
Max number of range bins	: 512
range resolution	: 150 m
No. of coherent integrations	: 4 to 512
Max number of FFT points	: 1024
Data type	: Raw Data / Spectral Data
Min height	: 1.5 km
Max height (clear air)	: 22 to 25 km
Mode of operation	: Doppler Beam Swinging

Table-2.1: Specifications of MST Radar

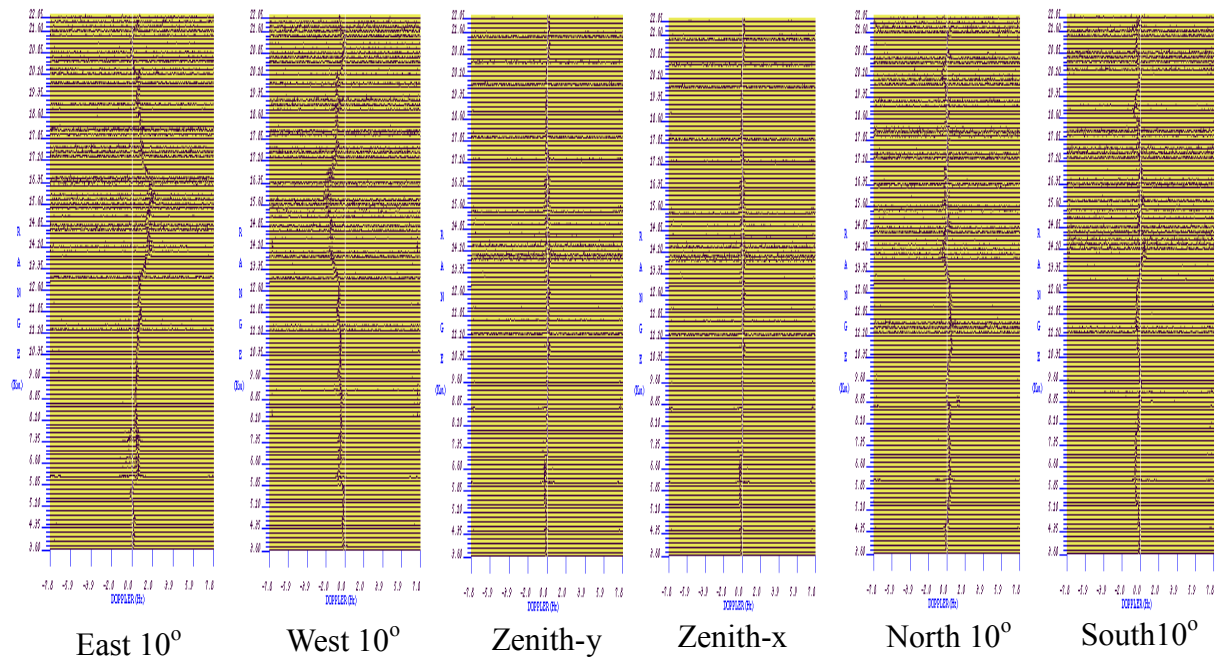


Figure-2.3: Typical range-Doppler Spectra obtained in five beam directions

Lower Atmospheric Wind Profiling (LAWP) radar

LAWP Radar consists of a simplified active micro-strip patch array, solid state TR modules, a passive two-dimensional beam forming network, which can generate 81 usable beams, a Direct-IF Digital receiver, a PC based Radar Controller. Most important feature of NARL LAWP is the active array configuration. In this configuration, which is shown in figure-2.4, each element of the planar microstrip patch antenna array is fed directly by dedicated low power solid-state transceiver module consisting of a power amplifier (PA) and LNA connected to the common antenna port through a circulator. A transmit/receive (T/R) switch switches the input port between the PA and LNA. These transceiver modules are made with commercially available communication components, making them low cost and affordable. Signal-to-Noise Ratio (SNR), thereby the range performance is significantly improved as the feed loss is eliminated. This configuration reduces the antenna size significantly (at least by a factor of 4-6) when compared to a conventional passive array system for the given range performance and makes the wind profiler compact and transportable. The second important feature of this system is the utilization of a low power two-dimensional passive multi-beam forming network, which simplifies the beam formation. This network distributes the radar exciter output signal and feeds the transceivers with appropriate amplitude and phase distribution. Beam switching is done by controlling a solid state single-pole-multi-through switch. Main advantage of the passive beam forming network is that it avoids the need for periodic phase calibration. In the receive mode, the outputs from the transceivers are appropriately weighted, phase shifted, combined in the beam forming network and delivered to the receiver. Other features include pulse compression scheme and direct IF digital receiver. Pulse compression scheme, incorporated into the system, enhances the height coverage without affecting the range resolution. Direct IF digital receiver is used for achieving better dynamic range, flexibility and programmability.

The photograph of the LAWP radar is shown in figure-2.5. Specifications are shown in table-2.2. Typical range-Doppler spectral plots are shown in figure-2.6.

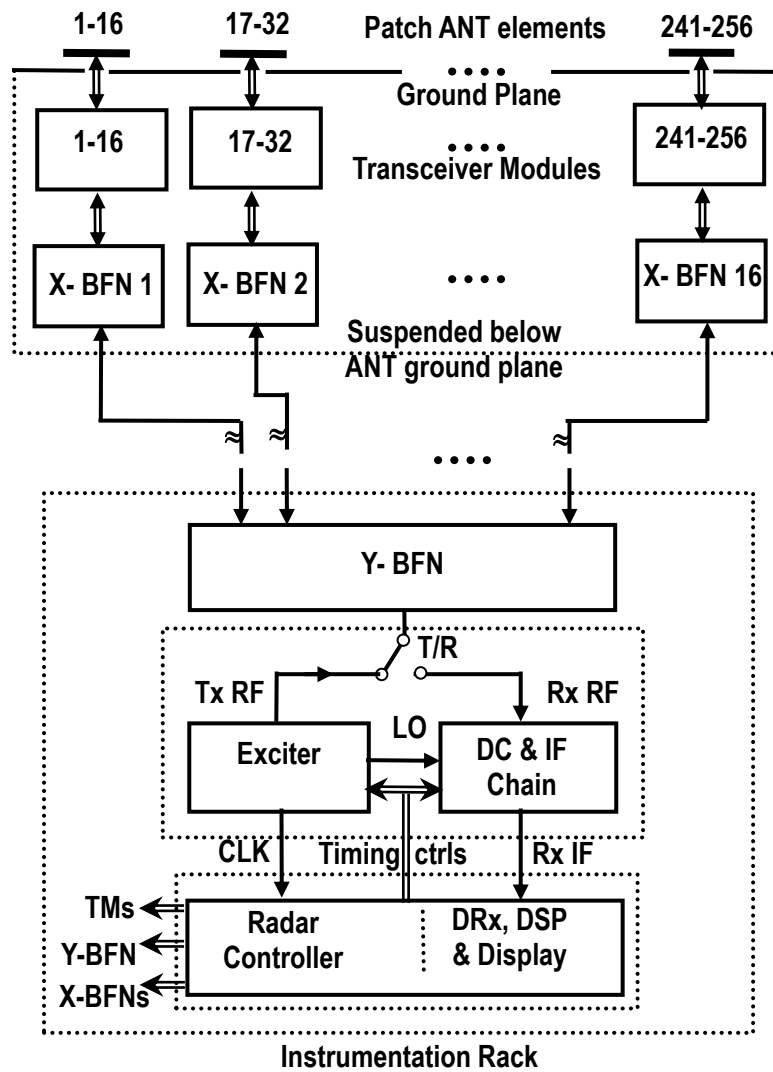


Figure-2.4: Block diagram of LAW P radar

Lower Atmospheric Wind Profiling Radar

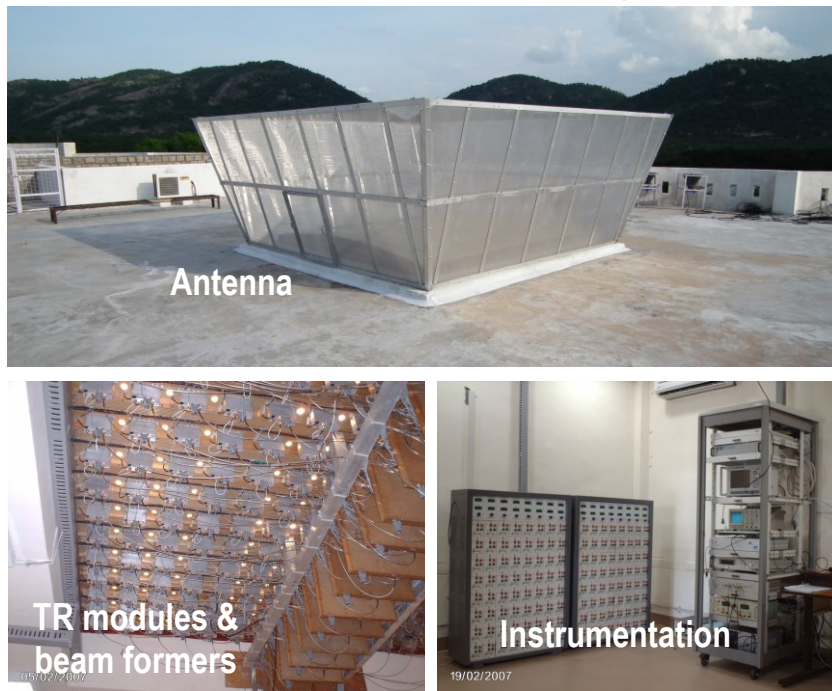


Figure-2.5: Photograph of the LAWP Radar

<u>Parameter</u>	<u>Value (2.8m/1.4m)</u>
Frequency	1280 MHz
Technique	Doppler Beam Swinging
Antenna type	Microstrip patch array
Array size	16x16
Beam width	4.5°
Beam former	Passive
No. of beams	81
Tx/Rx type	Solid state transceivers (256)
Peak power	2.5 kW
Duty ratio	Upto 10 %
Pulse width	0.25 – 8.0 μ s
NCI	4 – 1000
NFFT	32 – 1024
Range bins	1-256
Receiver	Super heterodyne
Detection	Direct IF digital
Min height	120 m
Max height	4-7 km

Table-2.2: Specifications of LAWP radar

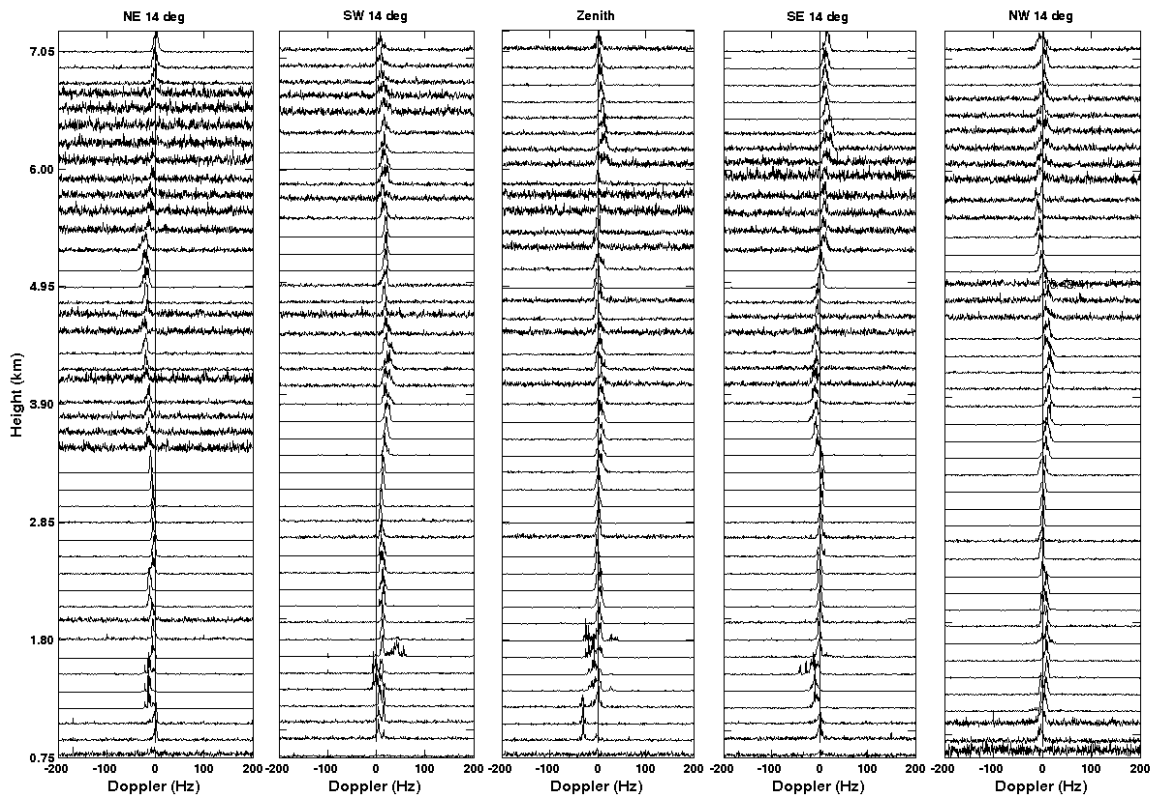


Figure-2.6: Typical range-Doppler spectra

CHAPTER-3

Data Processing

Back scatter from the clear air turbulence is a weak scattering mechanism, and thus the signal received from the atmosphere is very weak, normally buried in the noise. A sequence of processing steps is used to extract the atmospheric echoes and to derive the height profile of the wind vector components. The sequence of data processing is shown in figure-3.1. The steps involved in the processing data, are described below. The data is processed range-bin/gate wise. Figure-3.2 shows the range-gating.

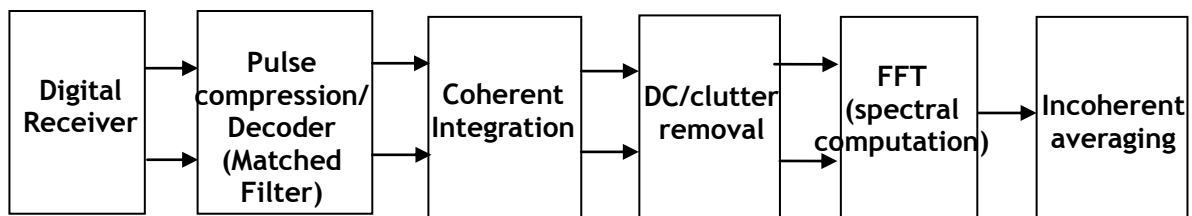


Figure-3.1: Data processing sequence

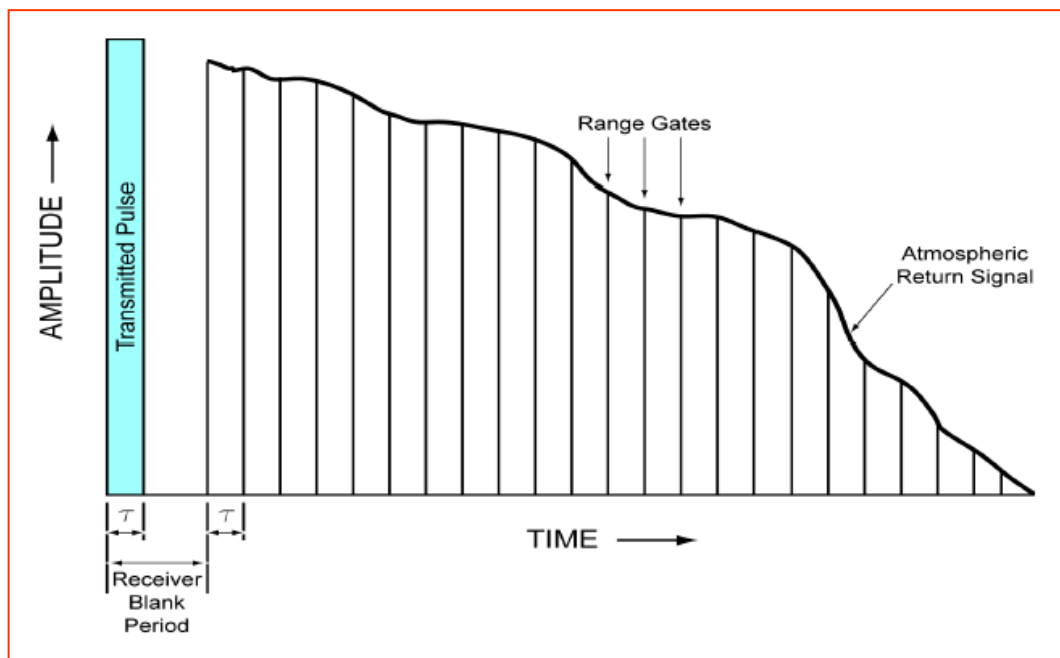


Figure-3.2: Range gating

Decoding (pulse compression): Pulse compression is a technique to achieve the maximum

height with better range resolution. It involves transmission of a long coded pulse, to get higher average power and processing the received echo to obtain a narrower pulse, which provides the better range resolution. In this technique, a long pulse is divided into N sub-pulses, each with a width equal to the baud length. The phase of each sub-pulse is chosen to be either 0° or 180° , based on a pre-defined code. Complementary codes are used in general which can provide better range side-lobe suppression. Two codes, of length N , whose ACFs have side lobes with equal magnitude and opposite phase. The sum of the two ACFs has zero side lobe level and peak with magnitude $2N$ and width equal to the baud length, thus achieving the better range resolution.

Coherent integration: The radar samples the atmosphere at every Inter Pulse Period ‘ T ’ and the unambiguous (or Nyquist) velocity of the radar is equal to $\pm\lambda/4T$, where λ is the radar wavelength. Since this gives a much larger range of measurable velocities than is needed, data rates in the subsequent processing stages are greatly reduced by performing time domain averaging (coherent integration). This process coherently averages the complex video samples from N consecutive pulses. This increases the sampling period and the unambiguous velocity is reduced to a practical value. Further this process improves the signal to noise ratio by N times. Reduction in data volume is another advantage. Coherent integration is shown pictorially in figure-3.3 and an example for a single range-bin is shown in figure-3.4.

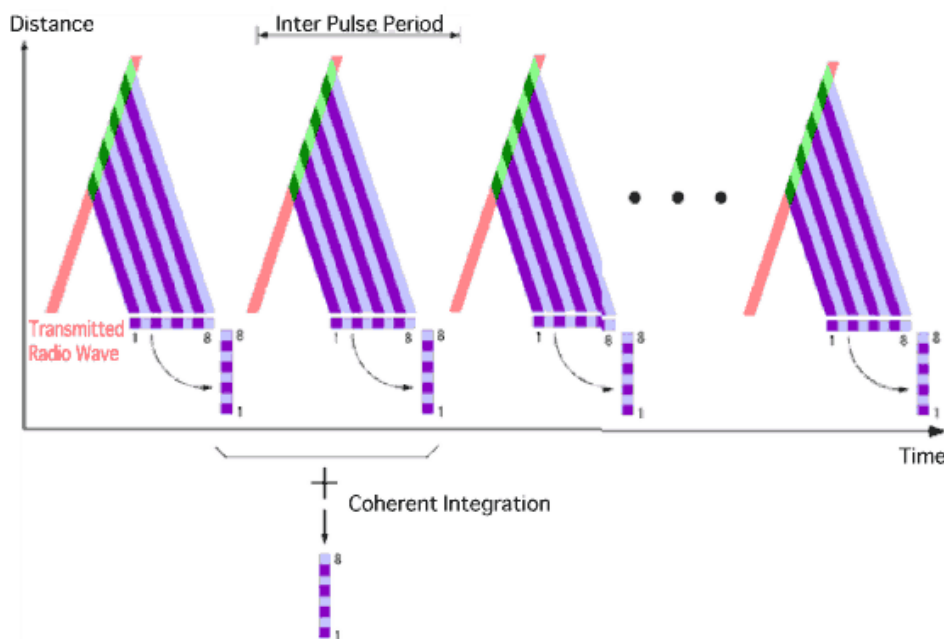


Figure-3.3: Range-bin wise coherent integration

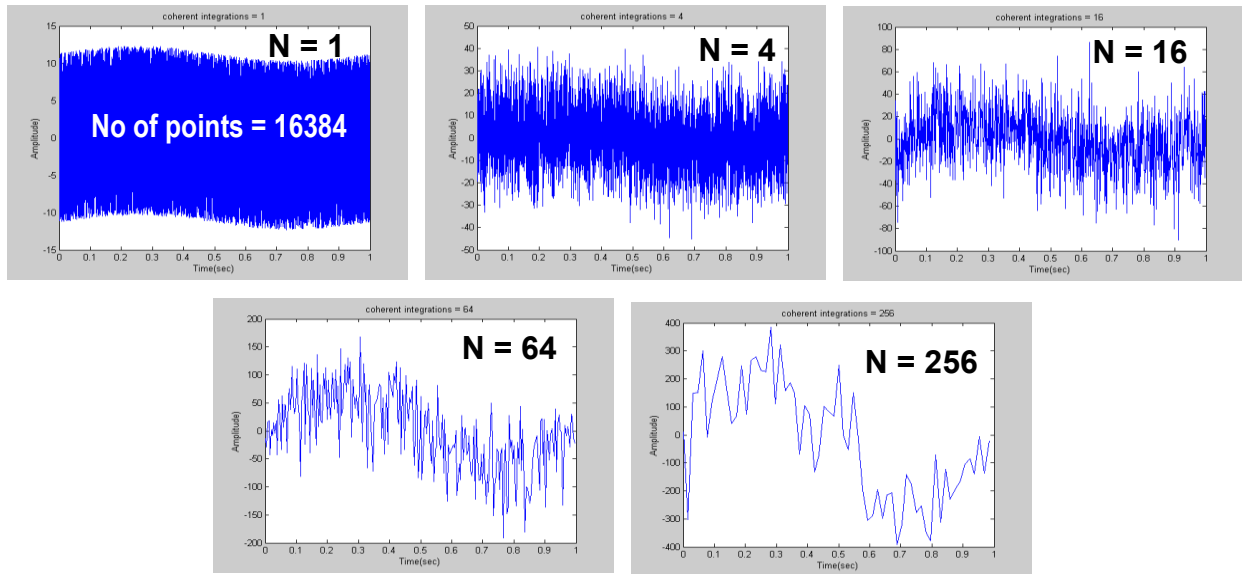


Figure-3.4: Coherent integration for a single range-bin: an example

DC/clutter removal: DC removal provides increased dynamic range by removing the average value of the signal. This helps to eliminate any fixed DC offset in the time domain complex signals. The inphase and quadrature signals are averaged separately and the respective mean values are subtracted. Unlike MST radars, LAWP radars suffer from clutter due to slowly varying undesired echoes like reflections from trees, power lines swaying in the wind etc. A technique called de-trending is used, in the time domain, to remove the low Doppler clutter along with the system DC component.

Power spectrum computation: Windowing is applied to the time domain data. Rectangular or Hamming or Hanning window can be used. The complex time domain data after windowing is converted into frequency domain by applying complex FFT and computing the power spectrum

Incoherent integration: Several successive spectra are averaged to improve detectability and also to improve the SNR as shown in figure-3.5.

Typical processed Doppler power spectrum for a single range-bin is shown in figure-3.6. Figure also indicates the moments (signal power, mean Doppler, spectral width) which are computed off-line/on-line.

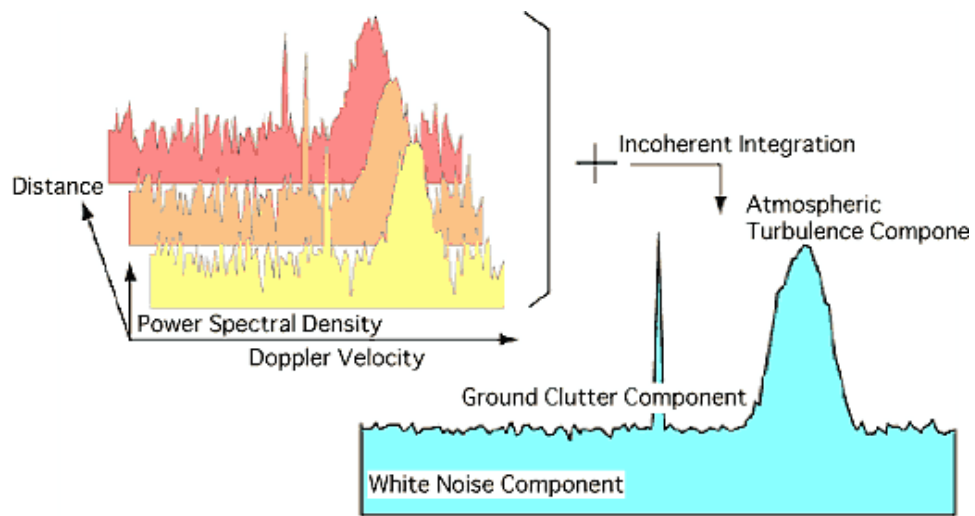


Figure-3.5: Incoherent integration

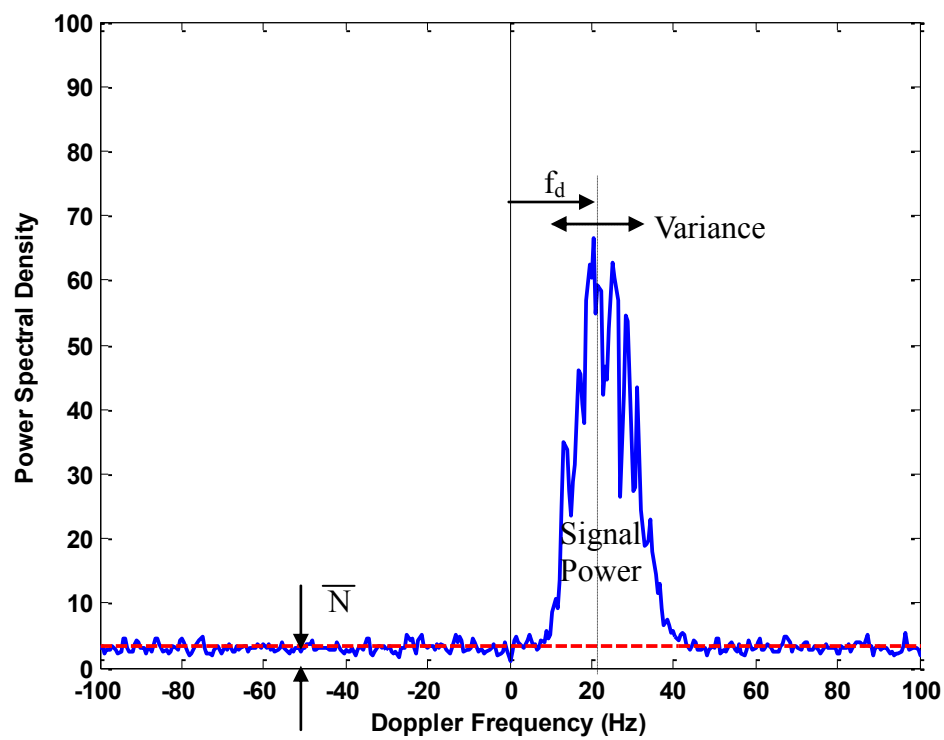


Figure-3.6: Typical Doppler power spectrum for a single range-bin

CHAPTER-4

Need for low cost radars/subsystems

DBS technique, which needs only a single receiver, is not suitable for situations, where the atmosphere is not homogeneous and disturbed. Such situations as convection, precipitation etc., demand radar techniques like spaced antenna, coherent radar imaging etc. These radar techniques require multiple receivers which needs to be spatially separated, to collect the backscattered echoes. Further, techniques like post beam steering, digital beam forming also need multiple receivers.

Wind profiling radars can be operated at several places over a geographical area to set-up a network of radars, which can be used for operational applications such as weather forecasting, nowcasting etc.

The above requirements give rise to the need for low cost radars/subsystems. The present work is developing a low cost digital receiver and data processing system, using a commercially available RTL2832U demodulator chip.

CHAPTER-5

RTL2832U: The low cost SDR

The RTL2832U is a high-performance DVB-T COFDM demodulator that supports a USB 2.0 interface. Modulation parameters, e.g., code rate, and guard interval, are automatically detected.

The RTL2832U supports tuners at IF (Intermediate Frequency, 36.125MHz), low-IF (4.57MHz), or Zero-IF output using a 28.8MHz crystal, and includes FM/DAB/DAB+ Radio Support. Embedded with an advanced ADC (Analog-to-Digital Converter), the RTL2832U features high stability in portable reception.

Though intended for decoding European HDTV broadcast in inexpensive USB dongle-type receivers, the fact that the RTL2832U chip can also output a raw digital stream describing the amplitude and phase (so-called I/Q data) of signals over a wide range of frequencies has made it a very cheap SDR.

Open source tools are used with this demodulator, which can translate I/Q information into audio and data streams. The result is a low-cost SDR that can pick up a huge variety of transmissions with different modulation schemes, including stereo FM from broadcasters, digital data packets from aircraft transponders, and single-sideband modulation (SSB) dispatches from amateur radio operators.

Because the receiver can see so much spectrum at once, we can use it to monitor activity on many channels simultaneously. The photograph of RTL2832U is shown in figure-5.1.

The salient features of RTL2832U are listed below.

- DVB-T COFDM demodulator
- Single low-cost crystal for clock generation (28.8 MHz, ± 100 ppm)
- USB 2.0 Interface
 - Supports USB Full/High speed
 - Configurable vendor information via external EEPROM

- Transfers raw (I & Q) data to PC
- Theoretical sampling rate is 3.2 MSPS.
- Frequency range depends on the tuner used. Dongles that use Elonics E4000 offer widest possible frequency range. (used in the present work)
- very cheaper (Rs 2000)
- Works as an SDR when software tools are used to convert the raw data output into audio or data streams

The limitations of RTL2832U are listed below

- The maximum sampling rate without loss of samples is found to be 2 MSPS.
- Not as sensitive as purpose built SDRs
- Not capable of transmitting a signal. Works only as a receiver.

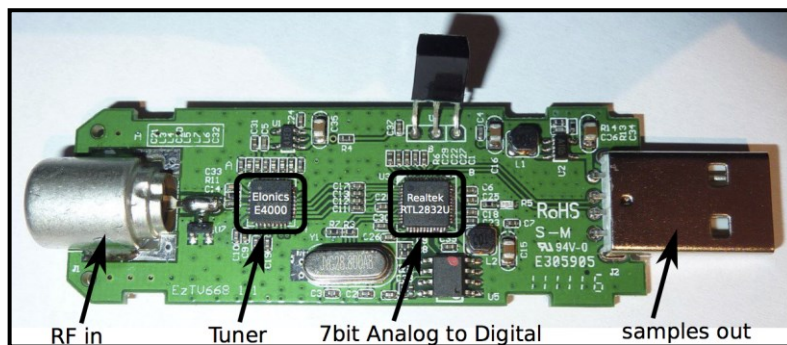


Figure-5.1: Photograph of RTL2832U demodulator

Requirements for the present application

- Several user-level packages like RTLSDR, HDSDR etc., are available that rely on the librtlsdr library which generally are used to test for the existence of RTL2832 devices and to perform basic data transfer functions to and from the device. To use it for advance experiments like the present application open source software tool named “GNU Radio” can be used.
- The receiver should be highly sensitive as the atmospheric echoes are very weak. As the sensitivity of the RTL2832U is poor, a receive front-end consisting of a Low Noise Amplifier, blanking switch and appropriate BPF, can be used to improve the sensitivity.
- The radar receiver must be a coherent receiver (i.e. the receiver clock must be

synchronized with the radar master clock). As the RTL2832U contains an in-built crystal and clock circuit, the frequency / phase difference between the radar clock and RTL2832U can be measured and compensated in the signal processing.

- Operation of the receiver should be synchronized with the radar transmission. As RTL2832U does not have a provision to accept any external trigger signal input from the radar, the transmit pulse leakage into the receiver can be used to detect the transmission. The location of the transmit pulse indicates the start of transmission and the receiver can be synchronized with this.
- The radar transmits for a small duration of the order of 1-16 μs and receives for duration of about hundreds of μs . As RTL2832U samples the data continuously, it is required to ignore certain number of samples corresponding to transmit pulse and blanking periods and use only the samples which lie in the radar receive window.

CHAPTER-6

GNU Radio

GNU Radio is a free & open-source software development toolkit that provides signal processing blocks to implement software radios. It can be used with readily-available low-cost external RF hardware to create software-defined radios, or without hardware in a simulation-like environment. It is widely used in hobbyist, academic and commercial environments to support both wireless communications research and real-world radio systems.

The signal processing blocks, which we can drag and drop, can generate data or read/write from/to in different formats, like binary complex values or WAV-files. The blocks include waveform generators, scope sink (oscilloscope), FFT sink (spectrum analyzer), file sink (output file), file source (input file), filters, channel codes, synchronisation elements, equalizers, demodulators, vocoders, decoders etc., which are typically found in radio systems. More importantly, it includes a method of connecting these blocks and then manages how data is passed from one block to another. The blocks are written in c++ programming language and Python language is used to combine signal processing blocks and to create flow-graphs. The type of data that can be passed from one block to another can be in bits, bytes, vectors, bursts or more complex data types.

Although initially created to run on Linux based operating systems (OS) for which there is currently more installation support, installation packages have now been developed for Windows and Mac operating systems. But as these packages cannot be used for the present application, Linux OS is used.

GNU Radio supports hardware units like Ettus Research USRP systems. It also supports RTL2832 TV tuners with the drivers gr-baz/osmocom which are available as third party modules. The RTL-SDR source block which is used to call RTL2832U demodulator in GNU radio, can be obtained by installing osmocom driver.

GNU Radio Companion (GRC) is a graphical tool for creating signal flow graphs and generating flow-graph source code. Figure-6.1 shows the GRC view.

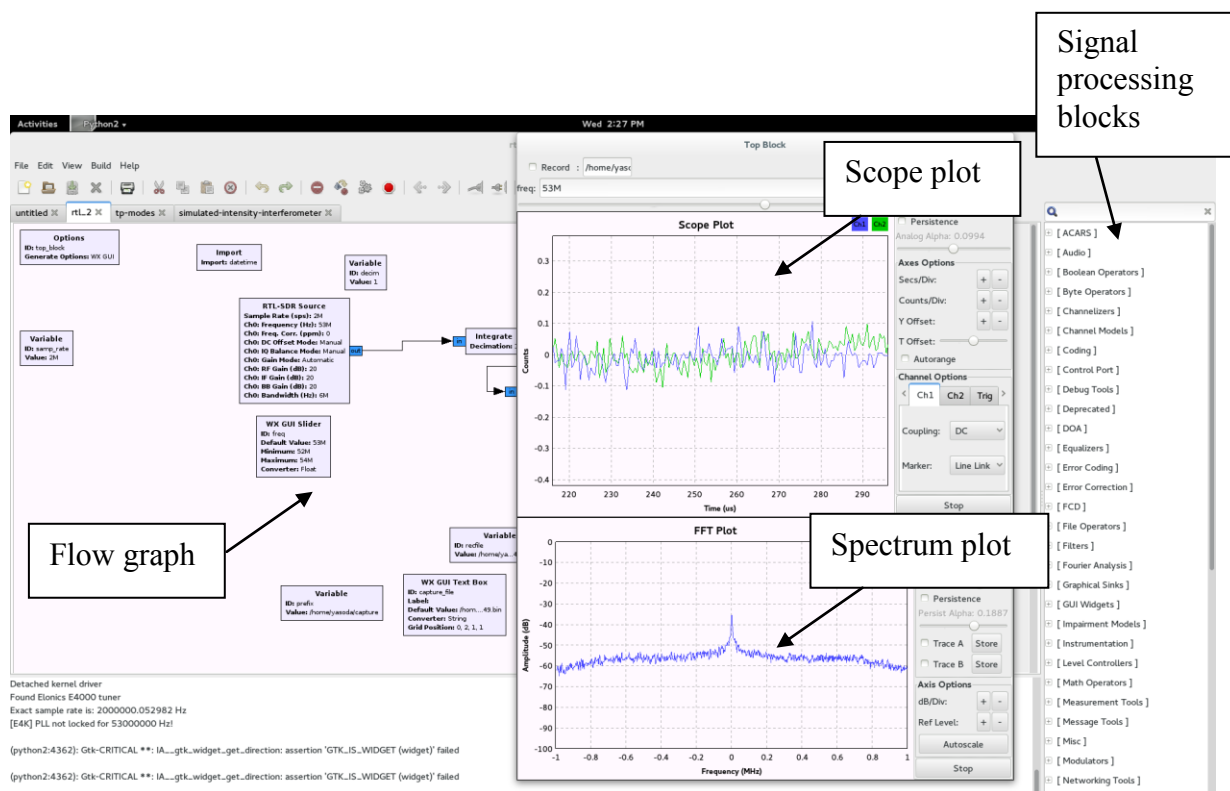


Figure-6.1: GNU Radio companion (GRC)

CHAPTER-7

Approach/realization

Initial Experiments: After procuring RTL2832 demodulator chip initially it is used for a couple of tests - First to monitor the spectrum which is present around us and then for listening to a local FM radio station. These two tests are explained below.

Monitoring the spectrum around

Initially RTL2832U is interfaced with PC by calling the RTL-SDR source block in GNU Radio. The sampling rate is set as 2 MSPS. The output is observed in scope sink and FFT sink. The frequency of RTL-SDR is tuned to receive the signal at different frequencies. It has shown the spectrum around and it is found that several interesting signals are present at different frequencies. Block diagram of the test for spectrum monitoring is shown in figure-7.1. The flow graph designed in GRC and the GUI for adjusting various parameters in RTL-SDR source block are shown in figure-7.2 and 7.3 respectively. Signal spectrum outputs at different frequencies are shown in figure-7.4. The photograph of the set-up is shown in figure-7.5.

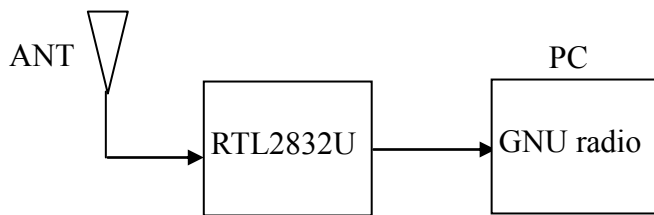


Figure-7.1: Block diagram of the setup

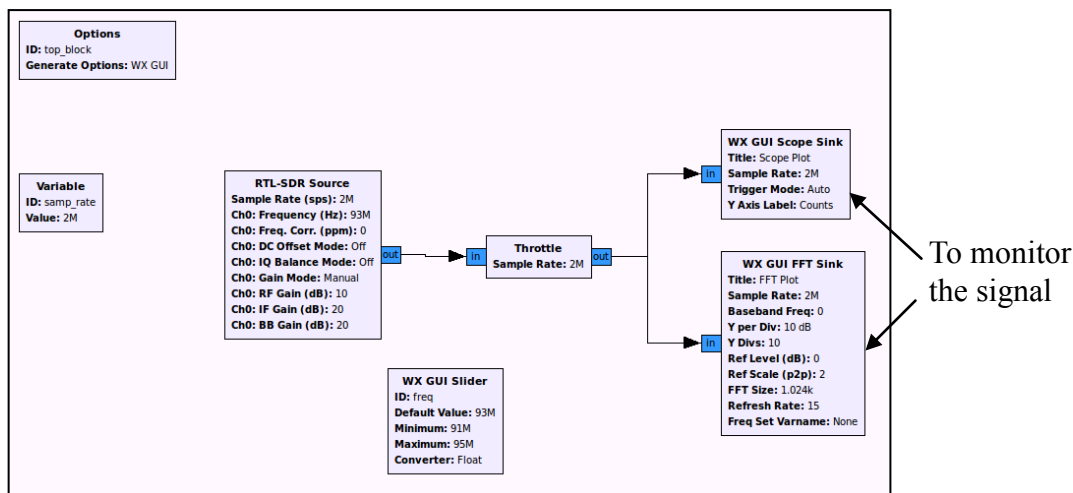


Figure-7.2: GRC flow graph to monitor the frequency spectrum

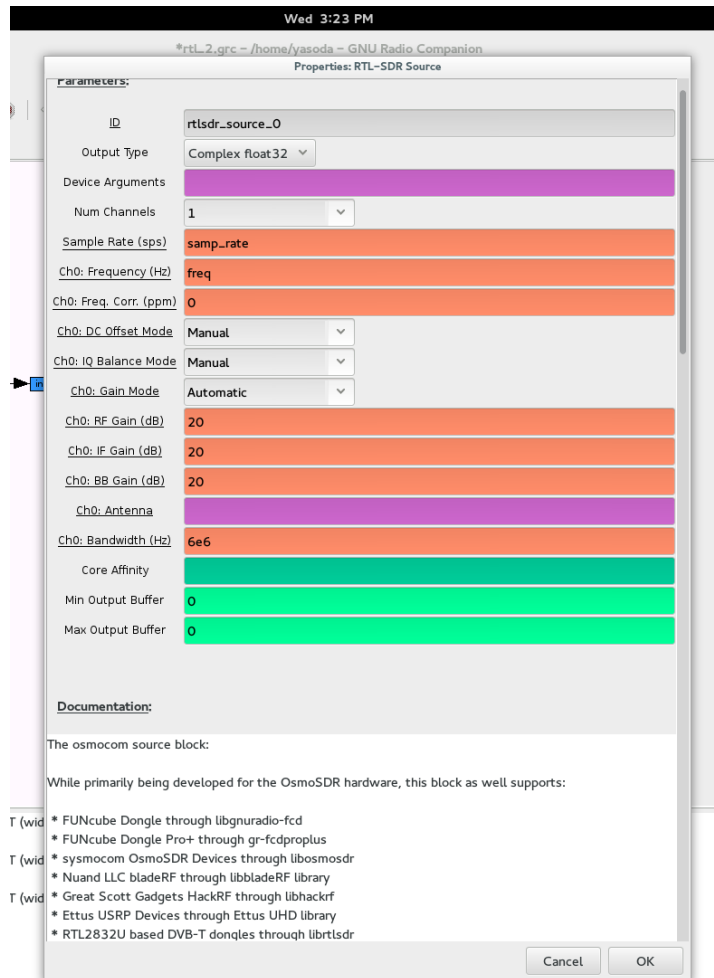


Figure-7.3: GUI for parameter adjustment

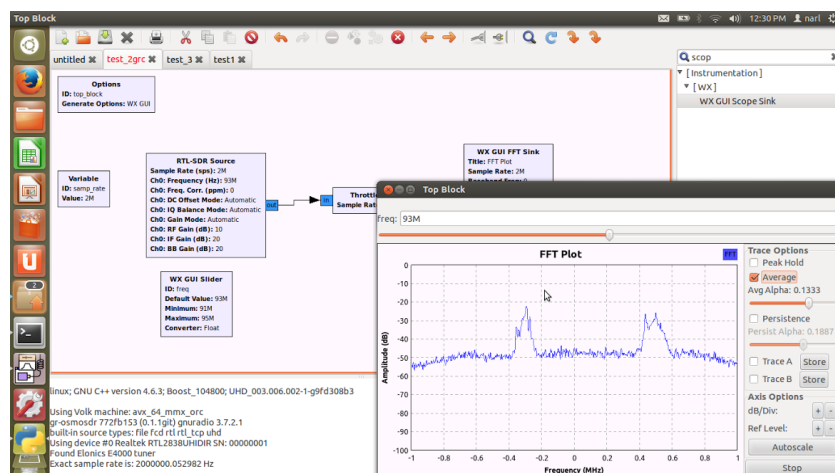


Figure-7.4 a: Spectrum showing FM Radio stations at 92.7 MHz and 93.4 MHz observed at Tirupati, Andhra Pradesh

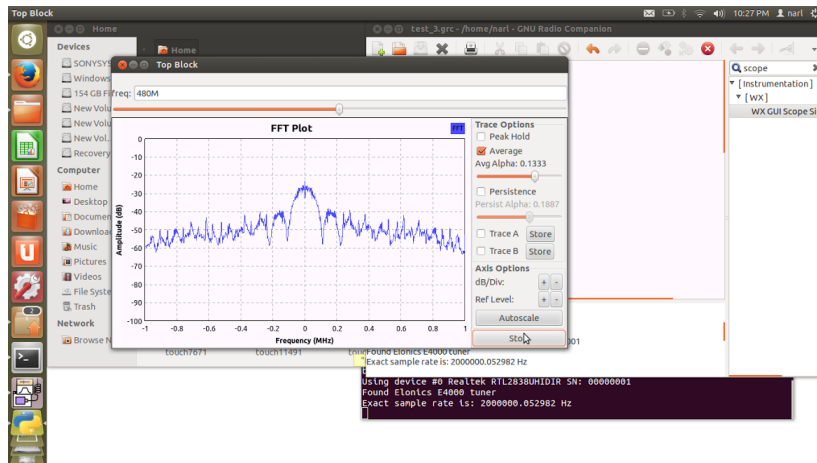


Figure-7.4 b: Spectrum showing a pulsed RF signal at 480 MHz observed at Tirupati, Andhra Pradesh

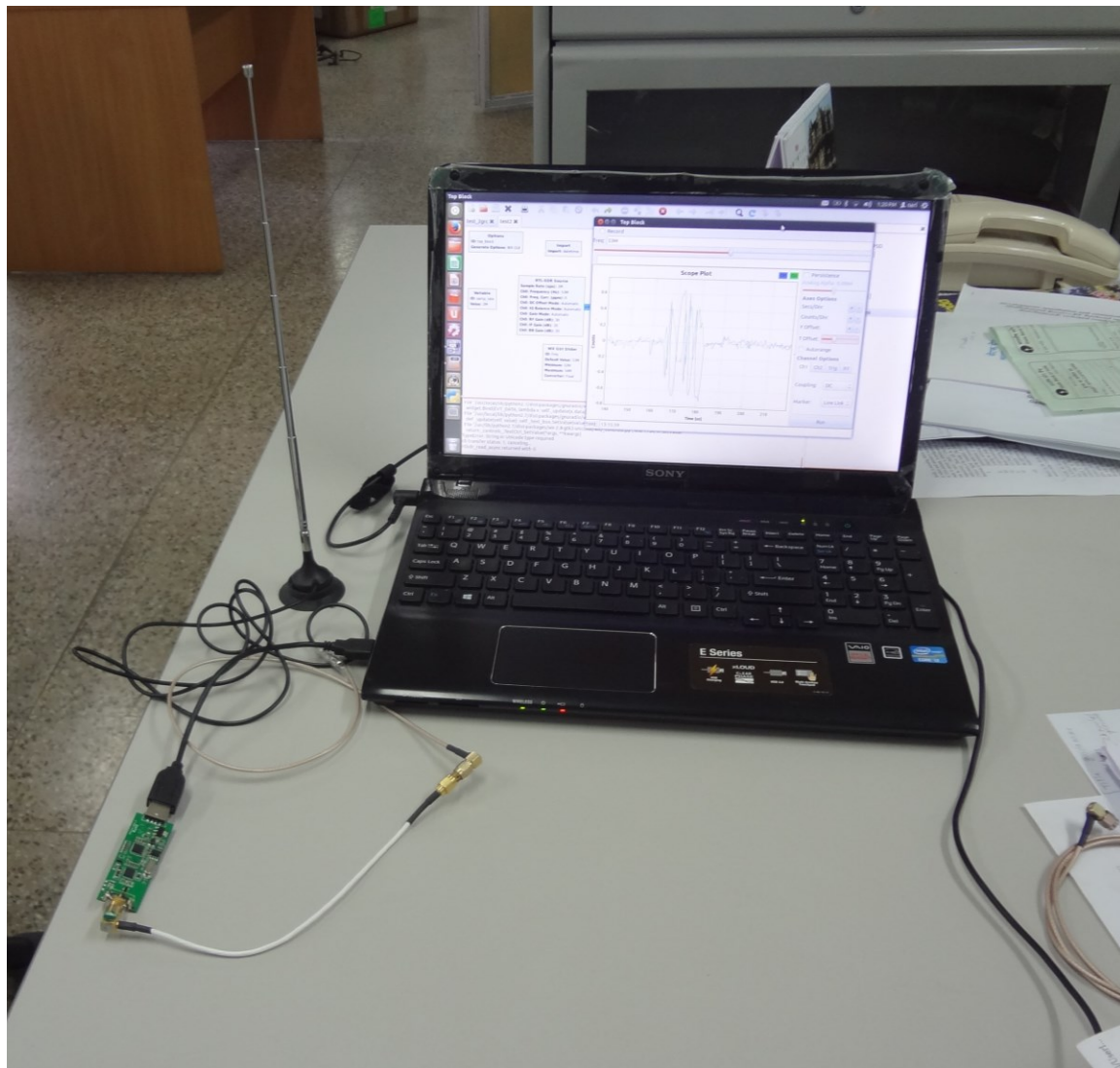


Figure-7.5: PHOTO of set-up

Listening to FM Radio station:

An FM Radio receiver is designed using the GRC with RTL2832U. The signal processing blocks for this test include RTL-SDR source, low pass filter, wide band FM receiver, rational resampler etc. Frequency of RTL-SDR block can be tuned to the local stations and can be listened. The set-up of this test is same as the previous test.

The flow graph designed for FM radio receiver in GRC is shown in figure-7.6.

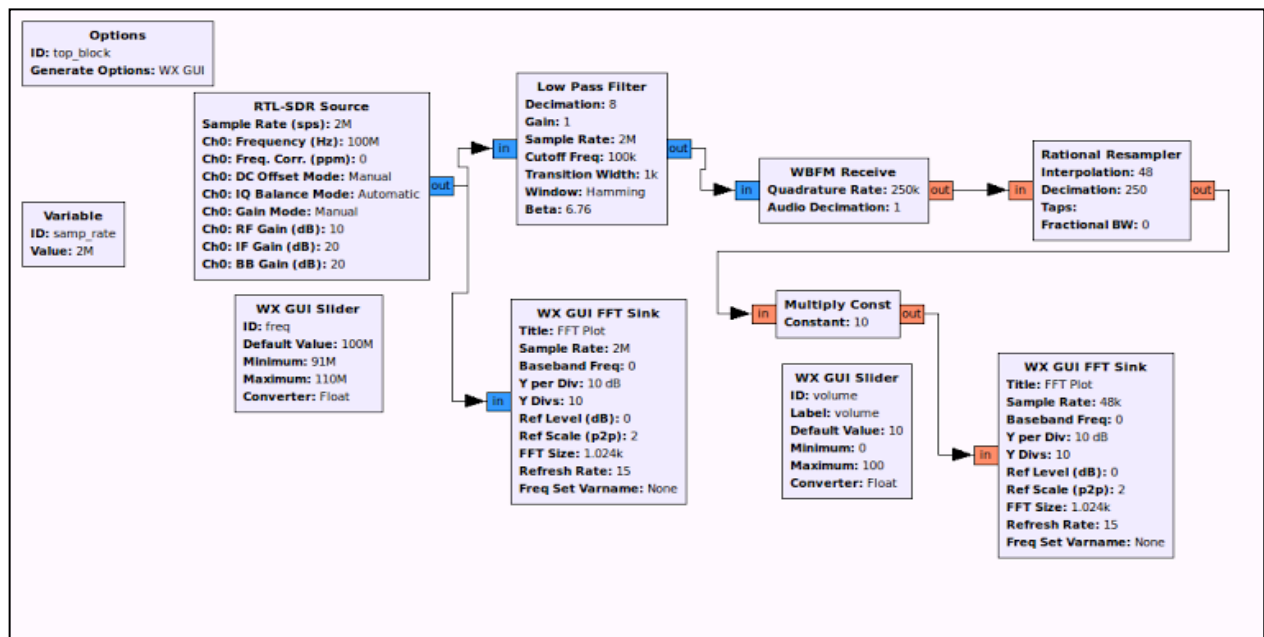


Figure-7.6: FM Radio receiver flow graph

Modifications and settings done to meet the application requirement

The RF connector which had come along with the RTL2832U demodulator can be connected only to the antenna that is supplied with it. This connector cannot be used to feed RTL2832U with signal from a signal generator as they have generally N-type RF connectors. Hence, the connector on the RTL2832U dongle is replaced with an SMA female connector (as it difficult to place an N-type connector there) and N-type RF adapters are used to feed signal from the signal generator and to connect to other equipment.

Set-up for signal generator experiment

Block diagram of the experiment for feeding the RTL2832U with a signal generator and the photograph of the experimental setup are shown in figure-7.7 a and 7.7 b respectively. A sinusoidal signal is fed from the signal generator to RTL2832U demodulator at 70 MHz. The frequency difference observed in the base-band signal at the output of RTL2832U is measured to be about 1.82 kHz in the scope plot of the GRC, as shown in figure-7.8. This difference can be nullified by adjusting the frequency of either signal generator or RTL-SDR source block. In this experiment the frequency of signal generator is adjusted (as 70.00182 MHz) to nullify the frequency difference. Figure-7.9 shows the scope plot of GRC after adjusting the frequency. It can be seen that the sinusoidal signal which was present before adjusting the frequency difference is eliminated after adjustment as can be seen from this plot.

A simulated pulsed RF signal at 70 MHz is fed to the RTL2832U demodulator. The pulse width is set at 4 μ s and the inter-pulse-period is set at 100 μ s. The output observed in the scope plot is shown in figure-7.10a. Base-band (I and Q) pulse output which can be used as timing reference can be seen in the plot. This experiment is repeated at 1280 MHz and the output time-domain and power spectrum plots are shown in figure-7.10b. The data output is stored in a binary file. An algorithm is developed in matlab to read the binary data file and to locate the rising edge of the first pulse in either I or Q data. This location provides the time stamp indicating the start of transmission. The algorithm makes use of the fact that the amplitude of transmit leakage pulse is larger than the amplitude of the receive/noise signal, making it distinct.

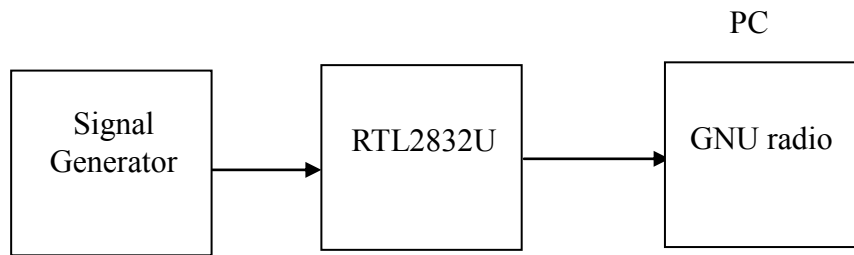


Figure-7.7a: Block diagram for the signal generator experiment



Figure-7.7b: Photograph of the signal generator experiment

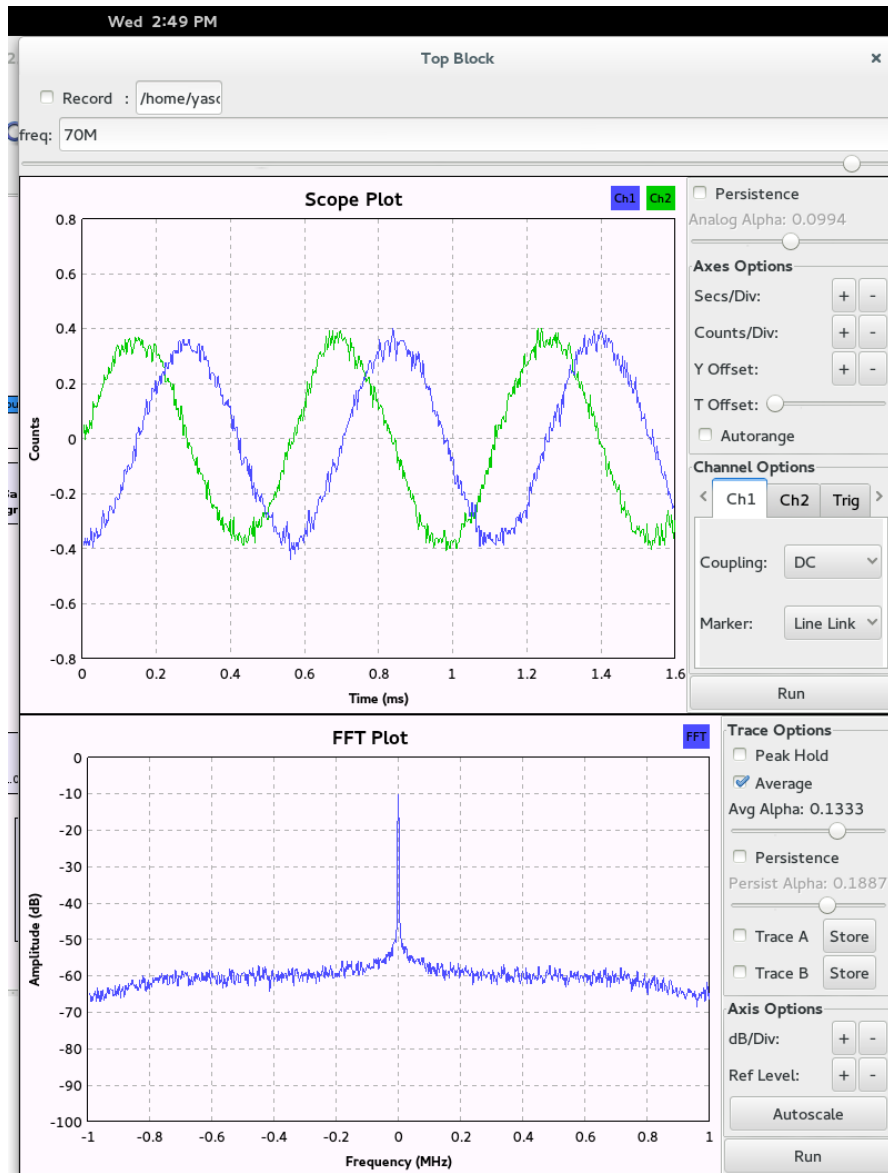


Figure-7.8: Base-band signal output showing the frequency difference between signal generator and RTL2832U demodulator.

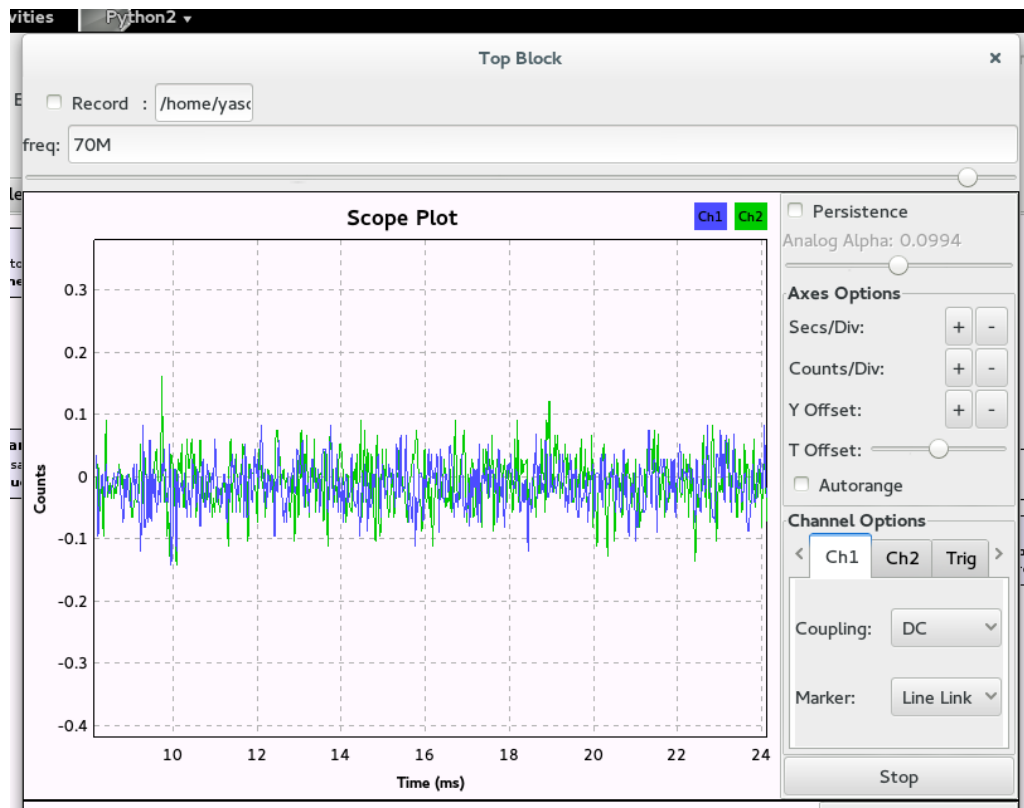


Figure-7.9: Scope plot of GRC after adjusting the frequency in signal generator (set to 70.00182 MHz)



Figure-7.10a: Base-band output for simulated 70 MHz pulsed RF

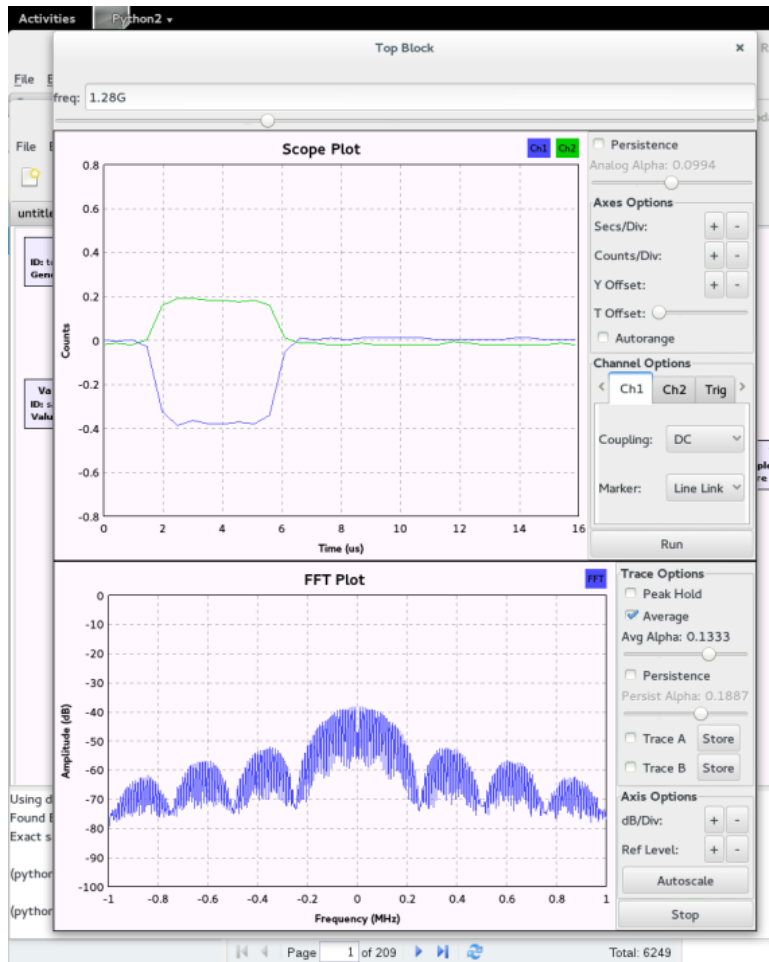


Figure-7.10b: Base-band output for simulated 1280 MHz pulsed RF with pulse width equal to 4 μ s. Nulls can be observed in the spectrum at 0.25 MHz corresponding to 4 μ s.

Experiments with LAWP radar

The RTL2832U is connected in the LAWP radar, operating at 1280 MHz, at the output of the back-end receiver. The back-end receiver has a down-converter, which converts the incoming atmospheric 1280 MHz RF signal into 70 MHz IF signal, IF amplifiers, appropriate switches and BPFs. Thus the signal given to the RTL2832U demodulator is the 70 MHz receive IF signal. Initially, the frequency difference between the radar 70 MHz IF and RTL2832U module is measured to be about 1.25 kHz. This frequency difference is adjusted by setting the frequency (as 70.00125 MHz) in the RTL-SDR source block. Experimental specifications of the LAWP radar are given in table-7.1. The data is stored in a binary file with date and time stamp. The flow-graph designed in GRC is shown in figure-7.11.

The data is processed using the matlab code. After locating the rising edge of the first transmit leakage pulse, a certain number of samples corresponding to the (Tx pulse+blanking period) are ignored. Then samples equal to the number of range-bins are picked. Again data samples are ignored from this point to the next transmit pulse, i.e. (IPP - receive window end). This process repeats and the code first arranges the data range-bin wise and then does the coherent integration and spectrum computation followed by incoherent averaging. The coherently averaged range-bin wise time series data (I & Q) and range-Doppler power spectra are shown in figure-7.12. From the figure it is observed there are strong spurious spikes present in the I & Q data which is not expected from the atmosphere. The radar experiment is repeated by changing the experimental parameters. But the I & Q plots are showing similar spurious spikes. This may be attributed to the two different independent clock sources used in the radar and the RTL2832U. This is confirmed with the simulated signal experiment from the signal generator given in the next section.

Parameter	Value
Pulse width	1 μ s
Inter-pulse-period	40 μ s
Coded/uncoded	Uncoded
Range bins	10
Coherent integrations	32

FFT (time series) points	512
Receive window start	750 m
Incoherent integrations	10

Table-7.1: Experimental specifications

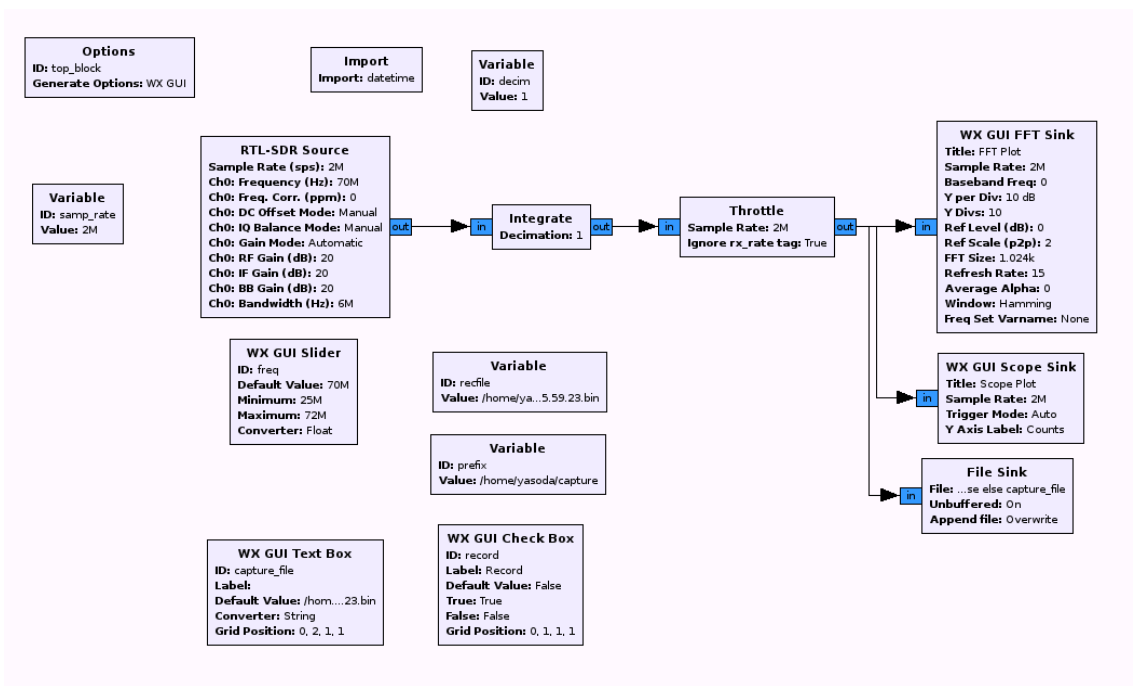


Figure-7.11: Flow graph for radar experiment

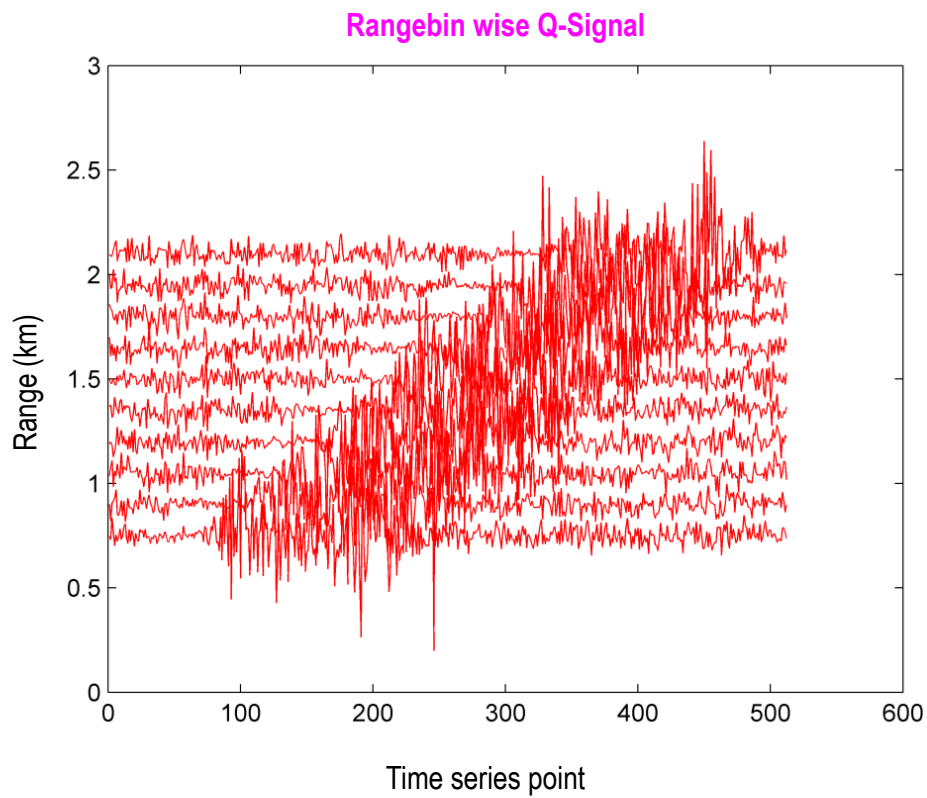
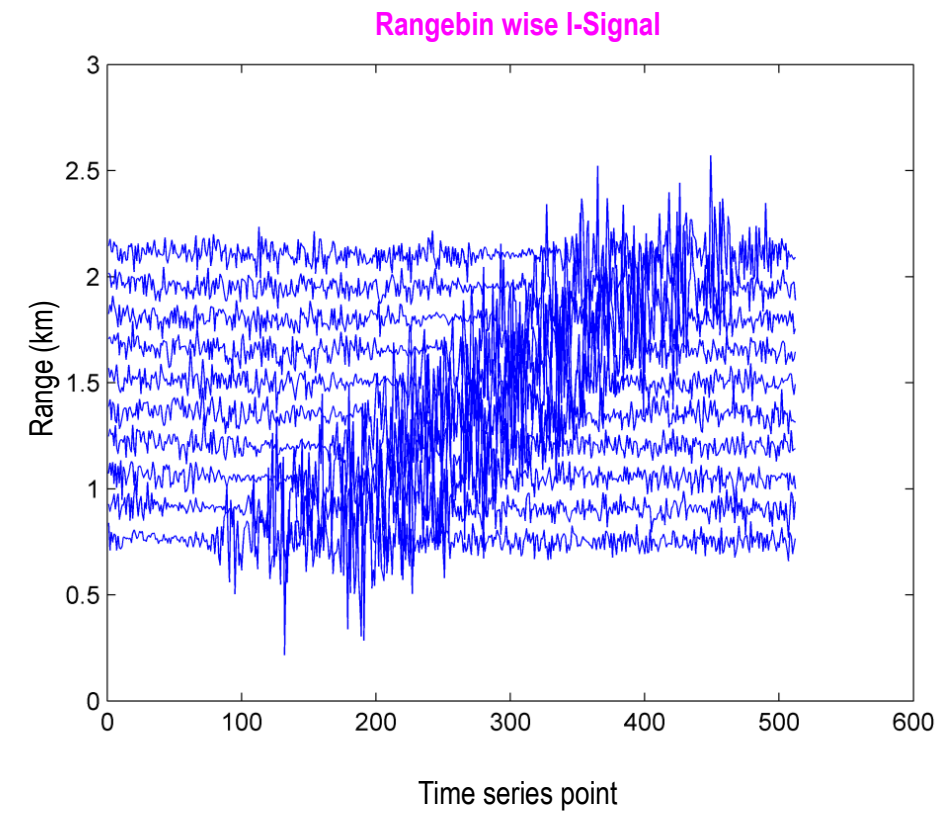


Figure-7.12a: I (top) and Q (bottom) plots indicating spurious spikes in the processed data

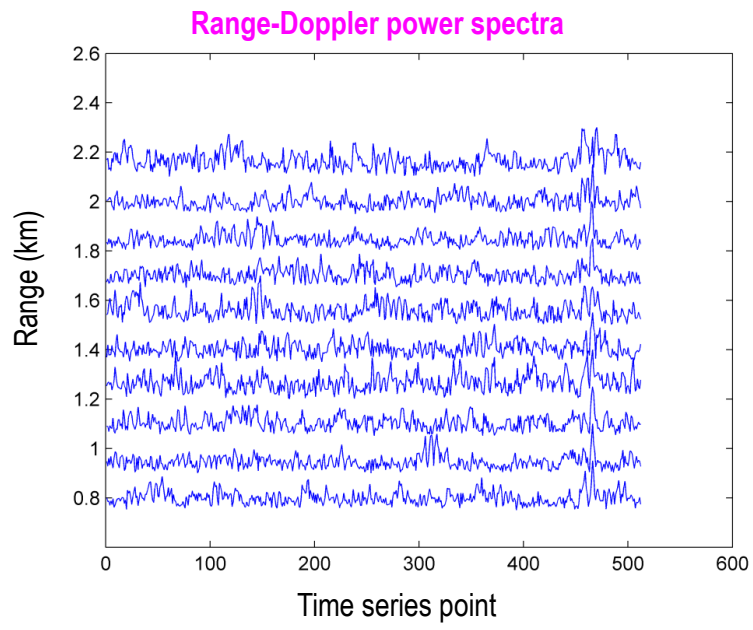


Figure-7.12b: Range-Doppler spectra for the data processed

Simulated signal experiment with the signal generator

A simulated pulsed RF signal at 70 MHz is fed to the RTL2832U module. The pulse width is set at 4 μ s and the inter-pulse-period is set at 100 μ s. The data is recorded into a binary file in GNU radio. The data is again processed using the matlab code and the I & Q plots, shown in figure-7.13, are observed. As the signal fed to RTL2832U is from the signal generator and as there is no atmospheric signal is present, ideally the receive period signal contains purely noise. Hence, the I & Q data should only contain noise values. But, the plots obtained with this experiment also are showing the spurious spikes similar to those obtained in the radar experiment. This confirms that this is due to the two different clocks of the radar and RTL2832U receiver.

Further, the raw data (I & Q data without any processing) obtained from RTL2832U receiver is plotted for several pulses. It was noticed that there is a sinusoidal signal modulating the base-band pulses, as shown in figure-7.14, though the frequency difference between the signal generator and the RTL2832U receiver are adjusted. The frequency of this modulating signal is measured to be about 40 – 50 Hz. This shows that the clock must be same for the signal generator and the RTL2832U to avoid the frequency difference between the two. The data is further checked for the position of the successive base-band transmit pulses. Each pulse should be at IPP*2 samples after the previous pulse. Initially the pulses are appearing at the correct indices. But, as proceeded further, this is not happening and the pulses are displaced from there correct time indices. The first pulse is at sample point number 34, as shown in figure-7.15. As the inter-pulse-period is 100 μ s, 835th pulse should occur at time index (sample point number) of 167034. But, from the figure-7.16, it can be seen clearly seen that the pulse is starting after 167040, indicating that there is a clear offset in the timing.

The above experiment indicates that the RTL2832U receiver clock must be synchronized with the radar master clock to avoid the spurious spikes in the processing. To overcome the timing offset problem, it was decided to change the clock circuit of the RTL2832U receiver.

An attempt was made to remove the crystal in RTL2832U and connect the clock signal from the signal generator, as shown in figure-7.17. But, with this modification, unfortunately, GNU radio did not detect the RTL2832U receiver. This is shown in GRC display of figure-7.18.

Hence, the crystal was restored back, which had made the GNU radio to detect it again. This indicates that removing the crystal is not the solution, rather the entire clock circuit needs to be replaced which can be locked to the external clock source, which will facilitate the RTL2832U receiver to be locked to the radar master clock.

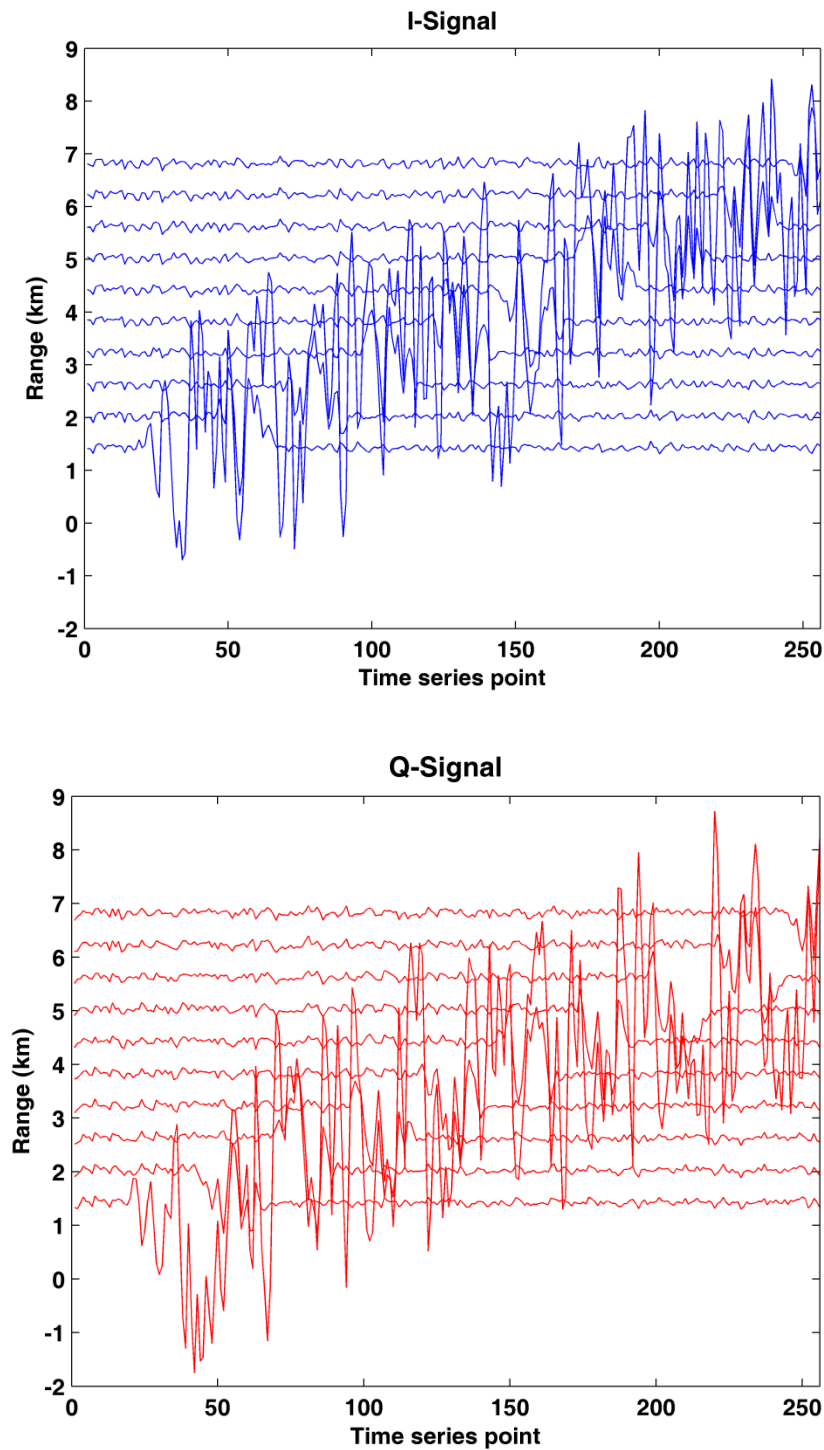


Figure-7.13a: I (top) and Q (bottom) plots indicating spurious spikes in the processed data

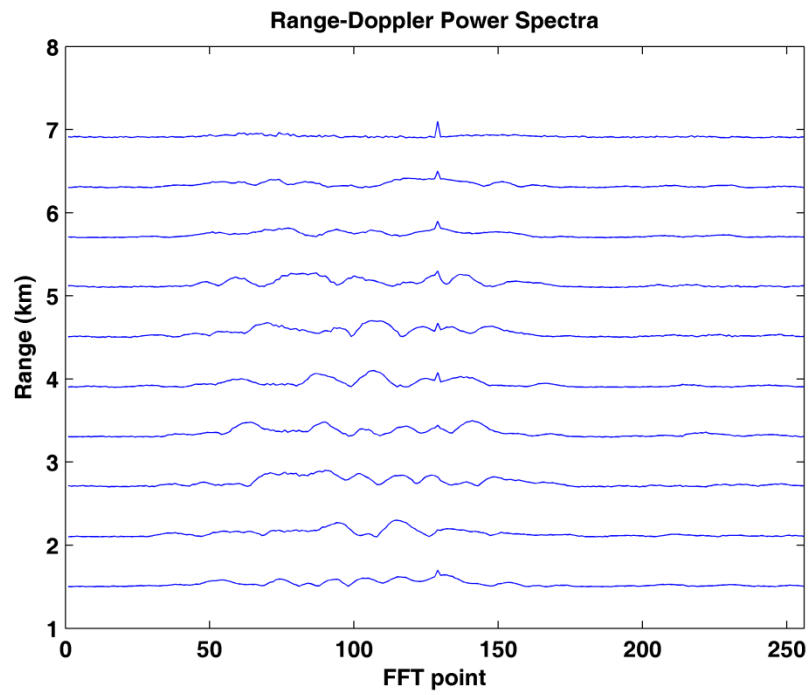


Figure-7.13b: Range-Doppler spectra for the data processed

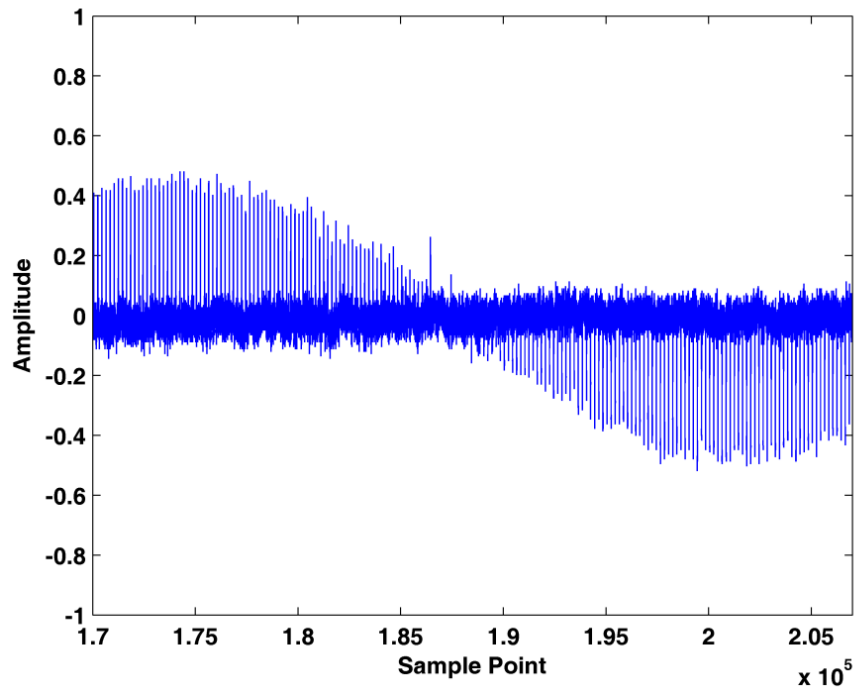


Figure-7.14: Raw base-band output of the simulated signal experiment, showing a sinusoidal signal modulating

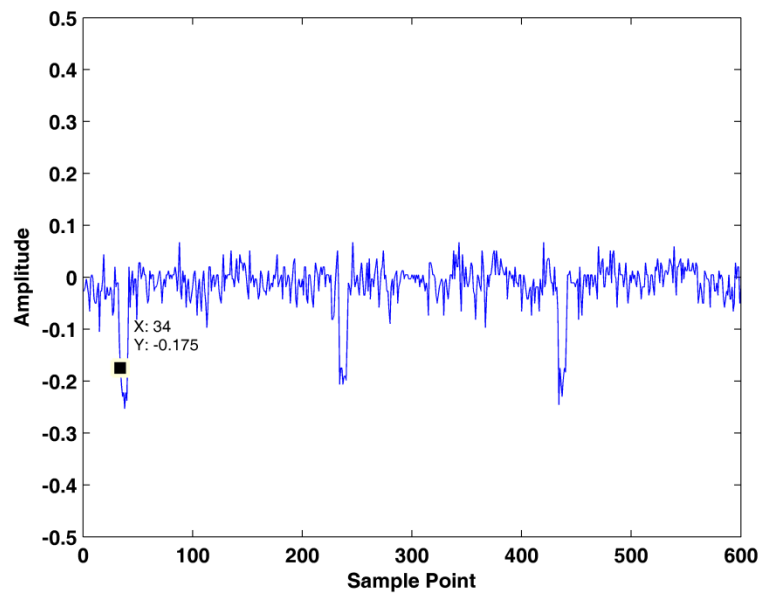


Figure-7.15: Base-band output of the simulated signal experiment indicating the start of first pulse.

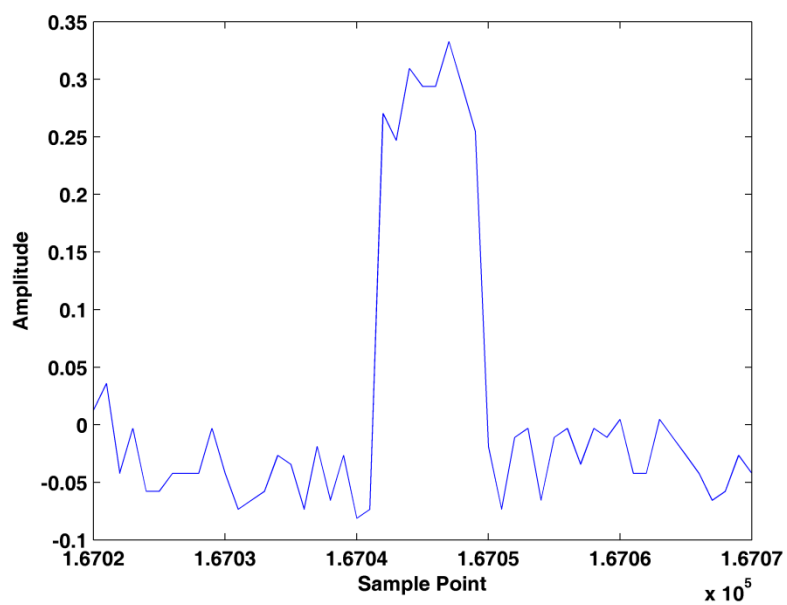


Figure-7.16: Base-band output of the simulated signal experiment showing the offset in timing

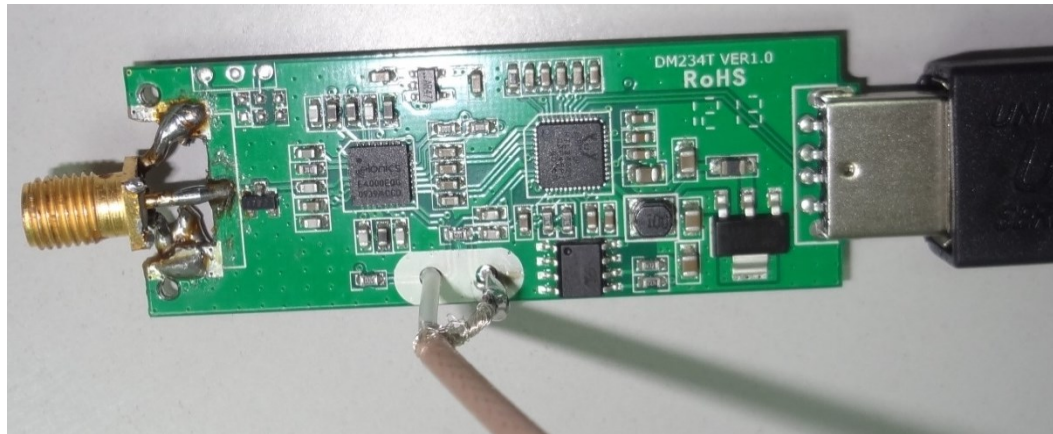


Figure-7.17: In-built crystal is replaced by an external clock. Figure also shows the replacement of the RF connector with an SMA connector.

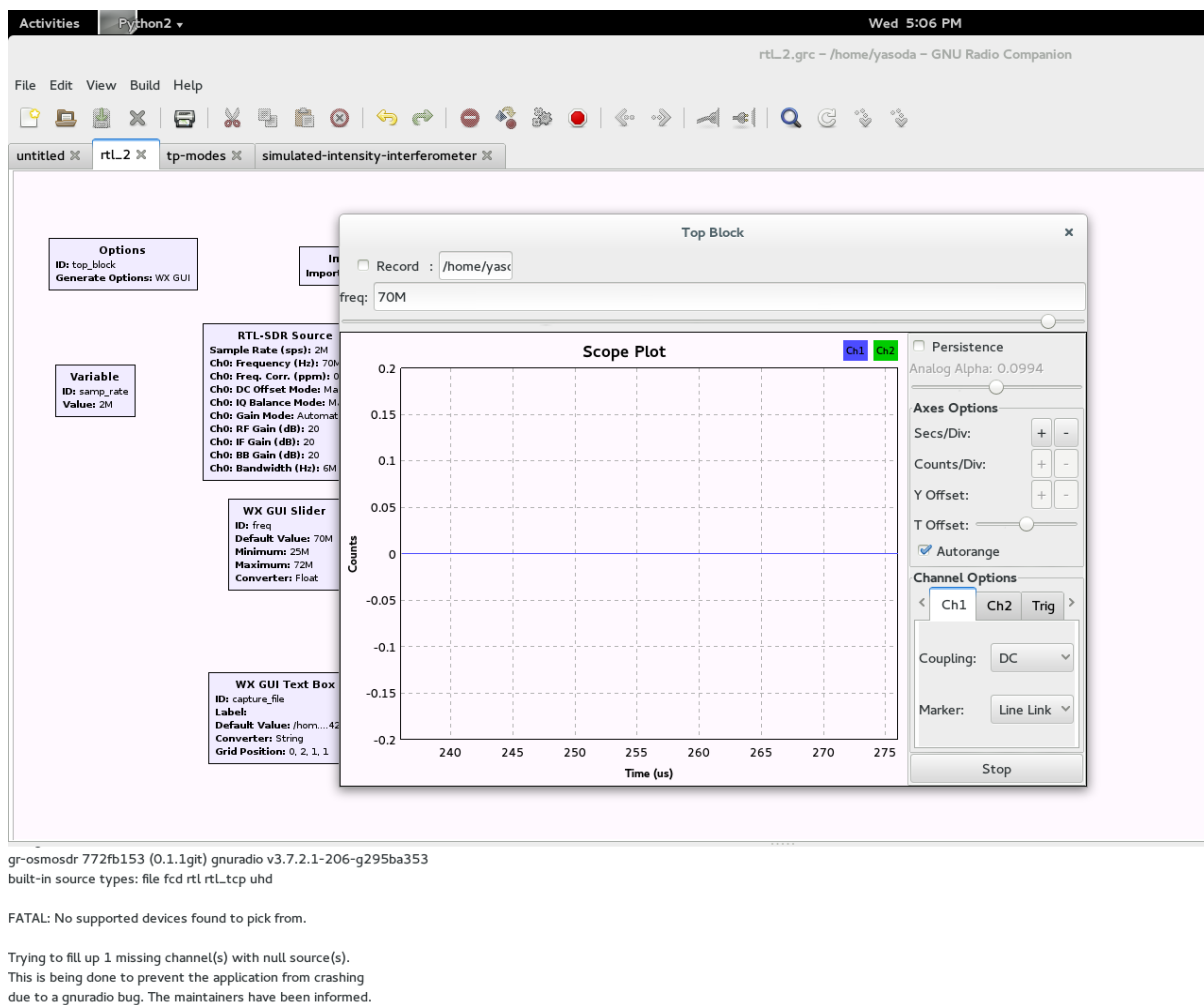


Figure-7.18: GRC screen when the RTL2832U is fed with external clock. No output in scope plot.

Conclusions

RTL2832U demodulator based low cost SDR is used to receive the radar return echoes. However, there is a difference in the clock frequency compared to the radar clock resulting in a timing offset in the data. Hence, it can be concluded that RTL2832U based low cost SDR can be used as wind profiling radar receiver provided the clock is locked to radar clock

The Tx leakage signal entering the receiver can be used to synchronize to the radar transmission. Rising edge of the Tx leakage pulse in the I/Q data is identified and used as the reference time for the start of radar operation and subsequent pulses are counted from this sample point.

Future scope

The clock circuit of the RTL2832U can be replaced with an external clock circuit, which is locked to the radar master oscillator. This will solve the timing offset problem, which is present in the current data. Possibilities can be explored to get the detailed configuration of the demodulator chip.

An algorithm can be tried to identify every leakage pulse and then pick the receive samples after it, instead of identifying the first Tx leakage pulse position and then counting the sample points to find the next pulse, to solve the spurious spikes in the I/Q data.

Presently a matlab code is written, to read the stored data file, to identify the Tx leakage pulse, pick the receive samples and do the processing, which is hard to use for real time applications. The same can be implemented in C/C++, which can be used in real time.

REFERENCES

- [1]. Radar Hand book, Merril I Skolnik, 2nd Edition, McGraw Hill, ISBN: 0-07-057913-X
- [2]. Indian MST radar: System description and sample vector wind measurements in ST mode, P B Rao, A R Jain, P Kishore, Balamuralidhar, S. H. Damle, G. Viswanathan, Radio Sci., Volume 30, Issue 4, pages 1125–1138, July-August 1995
- [3]. Simplified Active array radar L-band for Atmospheric wind profiling: Initial results, P Srinivasulu, P Yasodha, A Jayaraman, S N Reddy, S Satyanarayana, 2011, J. Atmos.Oceanic Technol., 28, 1436-1447.
- [4]. <http://gnuradio.org/redmine/projects/gnuradio/wiki>
- [5]. <http://spectrum.ieee.org/geek-life/hands-on/a-40-softwaredefined-radio>